



FRIEDRICH-SCHILLER-
UNIVERSITÄT
JENA

Optimization-inspired Barriers in Nested Sampling

M A S T E R ' S T H E S I S

in fulfillment of the requirements for the academic degree of

Master of Science (M.Sc.)

in the study program 'Computational and Data Science'

FRIEDRICH SCHILLER UNIVERSITY JENA

Faculty of Mathematics and Computer Science

submitted by Farin Lippmann

born on the 02.02.2000 in Gera

Supervisor: Prof. Dr. Michael Habeck

Jena, Datum Hier

Zusammenfassung

Nested Sampling ist ein Algorithmus zur Anpassung von parametrischen Modellen in der Bayesschen Statistik. Der aufwändigste Schritt im Nested Sampling ist das likelihoodbeschränkte Sampling des Priors. Hier wird zufällig von dem Teil des Priors gezogen, dessen Likelihood oberhalb eines bestimmten Werts liegt. Standardmethoden wie Markow-Chain-Monte-Carlo-Verfahren sind hier dadurch limitiert, dass sie die Likelihood-Grenze erst dann bemerken, wenn sie bereits überschritten wurde. In dieser Arbeit stelle ich Nested Sampling mit Barrieren vor; eine Methode, welche die Idee einer logarithmischen Barrierefunktion aus der konvexen Optimierung in Nested Sampling integriert, um das likelihoodbeschränkte Sampling des Priors gezielt zu lenken. Dieser Ansatz erreicht in durchgeführten Tests im likelihoodbeschränkten Sampling des Priors Akzeptanzraten, die bis zu einem Faktor von 1,23 über der von Standard-Nested-Sampling liegen.

Abstract

Nested Sampling is an algorithm for fitting Bayesian statistical models. The most computationally expensive step in Nested Sampling involves sampling from the part of a prior distribution whose likelihood lies above a certain value, called likelihood-restricted prior sampling. Standard methods like Markov Chain Monte Carlo can be used for this step, but are limited by not noticing the likelihood constraint boundary until they have crossed it, causing low acceptance rates of proposals. In this thesis, I propose Nested Sampling with Barriers, a method that incorporates the idea of a log barrier from convex optimization into Nested Sampling to guide the likelihood-restricted prior sampler. In a conducted benchmark, this approach achieves acceptance rates during likelihood-restricted prior sampling that are up to a factor of 1.23 higher than those of standard Nested Sampling.

Table of Contents

Introduction	5
1 Background	6
1.1 Bayesian Statistics	6
1.2 Fitting Bayesian Models	10
1.2.1 Analytical and Numerical Quadrature Methods	10
1.2.2 Monte Carlo Methods	11
1.2.3 Markov Chain Monte Carlo Methods	12
1.3 Nested Sampling	13
1.3.1 From a Multi- to a One-Dimensional Integral	13
1.3.2 Sampling and Sorting	16
1.3.3 Introducing a Likelihood Constraint	19
1.4 Likelihood-Restricted Prior Sampling	23
1.4.1 Rejection Sampling	23
1.4.2 Discretized LRPS	23
1.4.3 Metropolis Algorithm	23
1.4.4 Hamiltonian Monte Carlo	25
1.5 The Barrier Method	27
2 Nested Sampling with Barriers	31
2.1 Motivation	31
2.2 Derivation	32
2.2.1 Deriving the Log Barrier Term	32
2.2.2 Incorporating the Log Barrier Term	33
2.3 Interpretation	38
2.3.1 Interpreting q	39
2.3.2 Influence of t and q_{\max}	39
2.4 Implementation of LRPS	40
2.4.1 Rejection Sampling and Discretized LRPS	40
2.4.2 Metropolis Algorithm	40
2.4.3 Hamiltonian Monte Carlo	40
3 Results	42
3.1 Nested Sampling with and without Barriers	42
3.1.1 Estimated Evidence	43

3.1.2	Posterior Modes Found	44
3.1.3	Number of Iterations	46
3.1.4	Acceptance Rate	46
3.1.5	Jump Distance	47
3.2	Influence of t and q_{\max}	49
3.2.1	Estimated Evidence	49
3.2.2	Posterior Modes Found	49
3.2.3	Number of Iterations	49
3.2.4	Acceptance Rate	49
3.2.5	Jump Distance	52
4	Conclusions	54
Bibliography		56
Appendix		59

Introduction

Bayesian models are widely used for statistical inference tasks. They can extract information from data in a way that leads to intuitively interpretable results. Fitting a parameterized Bayesian model comprises more than just computing a point estimate for the parameter values, as would be the case with a maximum likelihood approach. Instead, the result of Bayesian inference comprises a whole probability distribution over the parameter space, called the posterior distribution. A distribution, as opposed to a point estimate, provides extra information about how sure we can be of the results of our inference. Bayesian inference also provides a canonical way to incorporate prior information about the model parameters, which the maximum likelihood approach does not.

The upsides of Bayesian inference come at the cost of being more difficult than maximum likelihood estimation, especially so with increasing model complexity. Many techniques have been developed for the purpose of Bayesian inference, the most common of which are Monte Carlo methods. Monte Carlo methods perform inference by sampling parameter values from the posterior distribution. Commonly used methods (Gibbs sampling [1], the Metropolis algorithm [2], Hamiltonian Monte Carlo (HMC) [3], Slice Sampling [4], etc.) all come with one downside: They focus purely on the posterior distribution of a model fit and do not compute the evidence. The evidence is a term that comes up in Bayesian inference. It is a useful quantity that can be used to compare whole classes of models with respect to how well they fit some data. Approaches that allow for computation of the evidence are, for example, Annealed Importance Sampling [5], Thermodynamic Integration [6], and Probabilistic Integration [7]. Another one is Nested Sampling, introduced by Skilling [8], which is the method this thesis focuses on.

Nested Sampling is a Monte Carlo method for Bayesian inference whose main objective is computing the evidence, although it can also generate posterior samples. Nested Sampling contains a step where samples have to be generated from a

likelihood-restricted prior (likelihood-restricted prior sampling or LRPS). This step is challenging [9, p. 9], with standard Markov Chain Monte Carlo (MCMC) methods struggling to achieve high acceptance rates of proposals, because they only notice the likelihood constraint boundary once they have crossed it. In this thesis, I propose a modified version of Nested Sampling which uses the idea of a log barrier from convex optimization to guide the crucial LRPS step of Nested Sampling. This log barrier softens the hard likelihood constraint boundary and lets the LRPS-sampler feel it earlier, which results in acceptance rates that are up to a factor of 1.23 higher than those of standard Nested Sampling.

I begin by recapping important background information about the methods and ideas this thesis is based on, including Bayesian statistics in general, the Nested Sampling algorithm and the Barrier Method for solving convex optimization problems. Following that, using inspiration from the Barrier Method, I derive Nested Sampling with Barriers as an alternative to the standard Nested Sampling algorithm. I then review some of the variables and parameters introduced by Nested Sampling with Barriers and analyze their effects on the algorithm. Finally, I present the results of a benchmark where basic Nested Sampling and Nested Sampling with Barriers were run in different configurations on a set of example problems.

1 Background

This chapter contains the background information necessary to understand the contributions of this thesis, namely Bayesian Statistics in general, Nested Sampling in particular, and the Barrier Method for convex optimization.

1.1 Bayesian Statistics

In this section, I introduce the basic principles of Bayesian statistics, including seeing probability as an extension of formal logic, generative models, and Bayesian updating using Bayes' rule.

In Bayesian statistics, probability is used to model uncertainty. Imagine we had a (possibly unfair) coin, with a certain inherent probability of landing heads (or tails) each time it is flipped. Let us call this inherent probability of landing heads $\theta \in [0, 1]$. If we, for example, knew that the coin was exactly fair, we could say $\theta = \frac{1}{2}$. Using the vocabulary of classical formal logic, we would say " $\theta = \frac{1}{2}$ " is true.

But since even the most accurately manufactured coin will have some microscopic asymmetries, bumps and ridges, we can never be sure of the coin's fairness. If we are not certain whether a statement is true or false, formal logic leaves us with no options. And if we cannot even meaningfully describe the flip of a coin, how should we expect to be able to examine complex systems like the weather, the spread of diseases, the development of ecosystems, etc. This is where probability as an extension of formal logic can help [10, p. 12]. We can express our knowledge of the coin's fairness by assigning a probability density to each possible value of θ . In doing so, we create a probability distribution over θ . If we knew nothing about the coin's fairness, we might assign every possible value the same probability density using a uniform distribution:

$$P(\theta) = 1 \quad \forall \theta \in [0, 1]$$

To make the example a bit more interesting, imagine we that from tossing similarly

shaped coins in the past, we would assume that it would land tails more often than heads. In this case, we might use a probability distribution like the following, which assigns lower values of θ a higher probability density:

$$P(\theta) = 2 \cdot (1 - \theta) \quad \forall \theta \in [0, 1]$$

A plot of this function can be found on the left side of Figure 1.1.

By representing the coin’s fairness using a parameter θ , we created a simple parametric statistical model. Statisticians would call our model generative, because by plugging θ into a Bernoulli-distribution, we can generate new samples from it, thereby simulating coin flips. When we equip a statistical model’s parameters with a probability distribution, as we did in the last paragraph, we give it what Bayesian statisticians would call a prior [11, p. 34]. It is called a prior since it encapsulates our beliefs about the model before we have seen any data that resulted from the process we are modeling (before we ever flipped the coin). The name giving process of Bayesian statistics is updating our beliefs about the model’s parameter values using Bayes’ rule, after seeing new data. Bayes’ rule prescribes how to integrate data D , originating from the process we are modeling, into our prior beliefs $P(\theta)$ to arrive at updated beliefs $P(\theta | D)$ (read “probability of θ given D ”) [11, p. 36]. It follows naturally from applying the product rule for probability to the joint probability of parameters and data, $P(\theta, D)$:

$$\begin{aligned} P(\theta, D) &= P(\theta) P(D | \theta) \\ &= P(D) P(\theta | D) \\ P(D) P(\theta | D) &= P(\theta) P(D | \theta) \\ P(\theta | D) &= \frac{P(D | \theta) P(\theta)}{P(D)} \end{aligned} \tag{1.1}$$

Bayes’ rule (Equation (1.1)) is made up of four parts. Let us take a closer look at each of them:

Likelihood: Given a generative model with parameters θ in some space Θ , and some data D originating from the process the model is representing, we call $P(D | \theta)$ the likelihood of θ , often written as $L(\theta)$. It is the probability of the data when the model uses a certain set of parameters θ . Note that when viewed as a function of θ , the likelihood is not a probability distribution, since it generally does not integrate to 1. In the following text, the natural logarithm of the likelihood will often be

abbreviated as $l(\theta) = \log(L(\theta))$.

Prior: Bayes' rule requires a prior distribution over the model parameters, $P(\theta)$, often written as $\pi(\theta)$. This represents beliefs we have about the parameter values before taking the data into account, which could be results from previous experiments or qualitative knowledge about the modeled process (like in our coin example) [11, p. 34 f.]. Priors like this may seem arbitrary or subjective, but they are required for Bayes' rule to work and have three positives:

1. They provide a way to incorporate known information about the problem, which can matter especially when there is little data.
2. With enough data, all but the most confident priors are overwhelmed and end up contributing little to the resulting posterior.
3. Non-Bayesian methods can often be shown to be equivalent to a Bayesian inference with a certain choice of prior [11, p. 36]. By putting our prior beliefs on display openly, they, like the model itself, become subject to the research process and scientific discussion instead of staying hidden.

Other authors prefer to write the prior as $P(\theta | M)$ to make explicit that it still depends on our choice of model. I omit the conditional for the sake of less cluttered formulas, but still want to call attention to this fact.

Evidence: I refer to the denominator of the right side of Bayes' rule, sometimes also called marginal likelihood, average likelihood or marginal density of the data, $P(D)$, as the evidence. It normalizes the product of prior and likelihood into a probability distribution and can also be written as follows:

$$P(\theta) = \int_{\Theta} P(D | \theta) P(\theta) d\theta = \int_{\Theta} L(\theta) \pi(\theta) d\theta \quad (1.2)$$

Often, it is abbreviated as Z . The evidence provides a measure of how well the model fits the data across all possible parameter values. Because it averages over all parameter values, overly complex models that require a very specific combination of parameter values to do well are penalized [11, p. 221]. This way, the evidence provides a means to compare models that automatically accounts for overfitting. In general, the evidence is a huge integral and hard to compute [11, p. 221]. Computation of the evidence is a major focus of this thesis.

Posterior: The main result of most Bayesian model fitting is the posterior probability distribution over the model parameters, $P(\theta | D)$. It represents our updated beliefs about the parameter values after having observed the data [11, p. 36].

Let us return to our coin example to illustrate Bayesian updating. Say we flip the coin five times and observe the sequence H T H H H, where “H” means heads and “T” means tails. The likelihood of any parameter value θ would then be $P(\text{H T H H H} | \theta)$. For example, the likelihood of $\theta = \frac{3}{4}$ would be $\frac{3}{4} \cdot \frac{1}{4} \cdot \frac{3}{4} \cdot \frac{3}{4} \cdot \frac{3}{4} \approx 0.079$. For comparison, the likelihood of $\theta = \frac{1}{4}$ would be $\frac{1}{4} \cdot \frac{3}{4} \cdot \frac{1}{4} \cdot \frac{1}{4} \cdot \frac{1}{4} \approx 0.0029$. We can see how the likelihood lets us rank parameter values by how well the data supports them (see also the right side of Figure 1.1).

Now we can use Bayes’ rule to obtain the posterior. For our simple, one-dimensional example we can approximate the posterior numerically by discretizing the θ -space and evaluating Bayes’ rule for each discrete point. More information on how this step is done in practice follows in the next section. For each value of θ , we compute the unnormalized posterior probability $L(\theta) \cdot \pi(\theta) = P(\text{H T H H H} | \theta) \cdot 2 \cdot (1 - \theta)$. In this simple example, the evidence can be computed analytically, but for most real-world problems, this will not be the case. Then, an approximate method of evidence computation has to be used. Because it is more similar to the methods for evidence computation used later in this thesis, we will use an approximate method here as well. For our example, the evidence (1.2) can be approximated using numerical quadrature: $Z \approx \sum_i L(\theta_i) \cdot \pi(\theta_i) \cdot \frac{1}{N}$, where N is the number of points we discretize the θ -space into. To get our posterior values, we divide each of the unnormalized posterior probabilities by the evidence. The posterior can be seen in the bottom image of Figure 1.1. Note how the posterior mode lands somewhere in between the prior and likelihood modes. The data updated our ideas of the coin’s fairness, but did not completely override them. If we get more data by tossing the coin a few more times, we can use the posterior we just computed as the prior of the next inference. The more data we collect and incorporate, the more “sure” our posterior will be of the true value of θ , becoming increasingly thin and spiky.

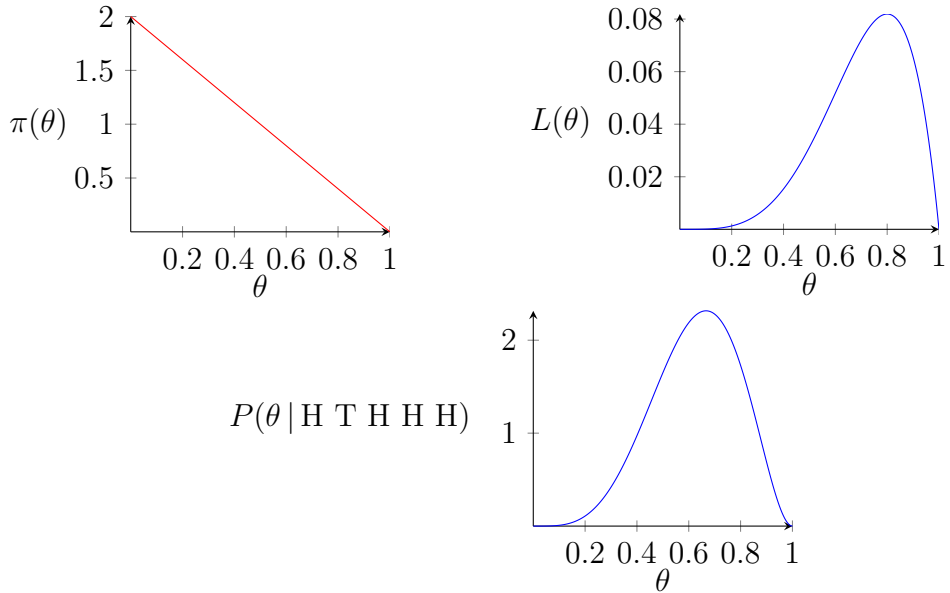


Figure 1.1: Prior $\pi(\theta) = P(\theta)$, likelihood $L(\theta) = P(HTH | \theta)$ and posterior $P(\theta | HTHHH)$ of θ in the coin example with $\pi(\theta) = 2 \cdot (1 - \theta)$ and data: H T H H H

1.2 Fitting Bayesian Models

Having introduced Bayesian statistics and described how Bayesian inference works conceptually, let us now turn our attention to how to do it in practice. This section briefly covers methods developed for fitting Bayesian models, starting with analytical and numerical methods, continuing to Monte Carlo methods and then Markov chain Monte Carlo methods.

1.2.1 Analytical and Numerical Quadrature Methods

In some cases, the posterior can be computed analytically, yielding a parameterized probability distribution. However, this only works for very simple models and severely limits the types of prior one can use (the prior has to be “conjugate” to the likelihood) [11, p. 39]. Another option is the one we used in the previous section, a numerical quadrature approximation utilizing a discretization of the parameter space. This approach does not work for models with many parameters, because its computational requirements scale exponentially with the dimensionality of the parameter space. For most real-world problems, both analytical and numerical quadrature methods are infeasible for the computation of the posterior.

1.2.2 Monte Carlo Methods

The most prevalent family of algorithms for Bayesian model fitting do not try to evaluate the posterior as a parameterized distribution, nor discretize the parameter space. Instead, they generate samples from the posterior distribution. These samples can then be used to approximate statistics (mean, variance, credible intervals, etc.) of the posterior distribution. Because of their probabilistic nature, algorithms of this type are called Monte Carlo algorithms.

Generating samples from a general probability distribution is still a difficult task. Especially for continuous distributions, where we cannot enumerate all possible values, there is no obvious way to do it [12, p. 358]. Another fact to consider is that we do not actually know the probability density function (PDF) of the distribution we want to sample from. Because we only know the likelihood and prior, but not the evidence (see (1.1)), we can only evaluate a function proportional to the posterior's density, an unnormalized version of it. All Monte Carlo methods for Bayesian inference have to solve this problem of sampling from a distribution while only being able to evaluate an unnormalized version of its density function.

To concretize the idea of Monte Carlo, I give a brief overview of one of the simplest Monte Carlo algorithms, Rejection Sampling, in the following paragraphs. Like most other Monte Carlo methods, Rejection Sampling makes use of a proposal distribution, a distribution we can easily sample from and which fulfills the following requirement: For a given unnormalized density function $P(\theta)$ of the target distribution, the proposal distribution's density $Q(\theta)$ can be scaled up using a constant c to fully envelop the target density:

$$c \cdot Q(\theta) > P(\theta) \quad \forall \theta \in \Theta$$

Then, we can generate a sample from the target distribution by sampling a θ^* from the proposal distribution and accepting the proposal with probability $\min\left(\frac{P(\theta^*)}{c \cdot Q(\theta^*)}, 1\right)$. If the proposal is not accepted, the process may be repeated until an accepted sample is found [12, p. 364].

While the simplicity of Rejection Sampling is appealing, it fails in practice because

1. we normally do not know the global maximum of our target distribution and thus do not know how to choose c , and
2. even if we did know how to choose c , the fact that in high dimensional problems typically only a small fraction of the parameter space carries high posterior

density forces us to scale Q so much everywhere else that acceptance rates plummet.

1.2.3 Markov Chain Monte Carlo Methods

The most used algorithms in Bayesian statistics overcome the flaws present in simple Monte Carlo methods like Rejection Sampling by choosing a proposal distribution with dependent samples. They are a subcategory of Monte Carlo methods called Markov chain Monte Carlo (MCMC) methods [13, p. 275 ff.]. Each MCMC sample is dependent on its predecessor and often lands in the vicinity of it. This allows more efficient exploration of the posterior, because once a region of high posterior density is found, its local surroundings often also carry high posterior density.

Again, to illustrate, let us take a look at one relatively simple example algorithm, the Metropolis algorithm [2]. The Metropolis algorithm uses a symmetrical proposal distribution $Q(\theta_{\text{new}} | \theta_{\text{old}})$. Often, a normal distribution around the last sample is used. The proposal is then accepted with probability $\max\left(\frac{P(\theta_{\text{new}})}{P(\theta_{\text{old}})}, 1\right)$ [12, p. 365f.].

I will not go into detail on why the Metropolis algorithm works, but I do want to at least mention the fundamentals of Markov chain Monte Carlo. Markov chain Monte Carlo methods get their name from the fact that their samples form a Markov chain. Markov chains are defined as a set of states Θ (in the case of Bayesian Inference these are all possible parameter values) with an initial probability distribution $P_0(\theta)$ over these states, along with a transition probability function $T : \Theta \times \Theta \rightarrow [0, 1]$ assigning a probability $T(\theta^* | \theta)$ to every transition from one state θ to another θ^* . This transition probability function satisfies $\int_{\Theta} T(\theta^* | \theta) d\theta^* = 1$. We can simulate a Markov chain by sampling an initial state $\theta_0 \sim P_0(\theta)$, then sampling the next state from the transition probability distribution $\theta_k \sim T(\theta_k | \theta_{k-1})$. We can also analyze the probability of being in a certain state after k steps [12, p. 372]:

$$P_k(\theta^*) = \int_{\Theta} P_{k-1}(\theta) T(\theta^* | \theta) d\theta$$

This also lets us define stationary distributions of Markov chains. These are the key to using Markov chains for sampling, because once a Markov chain finds its way into a stationary distribution, it stays there. We call $\mathcal{P}(\theta)$ a stationary distribution of a Markov chain if the probability of being in a state θ^* can be computed by integrating over the probabilities of being in any other state and transitioning to θ^* [12, p. 372]:

$$\mathcal{P}(\theta^*) = \int_{\Theta} \mathcal{P}(\theta) T(\theta^* | \theta) d\theta \quad \forall \theta^* \in \Theta$$

MCMC methods focus on cleverly defining their transition probabilities in such a way that the target distribution is the only stationary distribution of the Markov chain. That way, when the chain is sampled for long enough, it eventually produces samples from the target distribution [12, p. 372].

Now that I've touched on the classical methods for Bayesian inference, I want to explain why there is room for improvement. As covered in Section 1.1, the evidence is an immensely useful part of Bayes' formula (Equation (1.1)) because it allows model comparison that accounts for overfitting. Most MCMC methods only generate samples from the posterior, they do not compute the evidence and thus lose out on its positives. Computing the evidence integral is generally a difficult task [11, p. 221]. Since the parameter space for real-world models is high-dimensional, with only a small fraction of this space containing meaningful posterior probability mass, numerical quadrature methods that discretize the space evenly fail. One might think to use the modes of the posterior as a guide, since posterior density concentrates around them, but the evidence is an integral, and integration accumulates not densities, but density times volume, or mass. In high dimensional spaces, most of the probability mass lies not at the modes, where there is high probability density, because it concentrates on very little volume. Instead, most probability mass is found further out from the mode, where there is still relatively high density, but spread over magnitudes more volume. For this reason, we cannot simply explore the posterior in a small region around the modes [14]. There are probabilistic integration methods like Bayesian cubature [7], that estimate the evidence from a set of given MCMC samples, which by definition concentrate where there is high posterior mass. However, this thesis focuses on a method whose main objective, from the start, is computing the evidence.

1.3 Nested Sampling

Nested Sampling, introduced by Skilling [8], is an algorithm that computes the evidence of a Bayesian model while also generating samples from the posterior distribution. In this section, I derive the Nested Sampling algorithm, explaining the main ideas along the way.

1.3.1 From a Multi- to a One-Dimensional Integral

We start by reducing the potentially multidimensional evidence integral from (1.2) to a one-dimensional integral. To this end, we first replace the likelihood in the evidence integral by its layer cake representation, a tool borrowed from measure

theory [15, p. 26]. For a quick derivation of the layer cake representation, let us define the indicator function $\mathbb{1}_S(x)$:

$$\mathbb{1}_S(x) := \begin{cases} 1, & \text{if } x \in S \\ 0, & \text{otherwise} \end{cases}$$

We will often use the indicator function with an abbreviated set notation. For some predicate $p : X \rightarrow \{\text{true, false}\}$, $\{p(x)\}$ is short for $\{x \mid x \in X, p(x)\}$, and $\mathbb{1}_{\{p(x)\}}(x)$ is 1 exactly when $p(x)$ is true. With these definitions we rewrite $L(\theta)$ as its layer cake representation:

$$L(\theta) = \int_0^{L(\theta)} 1 d\lambda = \int_0^\infty \mathbb{1}_{[0, L(\theta)]}(\lambda) d\lambda = \int_0^\infty \mathbb{1}_{\{L(\theta) > \lambda\}}(\theta) d\lambda$$

The last equality holds because the integrand is still 1 for all values of λ that are smaller than $L(\theta)$ and 0 for all $\lambda > L(\theta)$. Now we plug this layer cake representation of $L(\theta)$ into the evidence integral:

$$\begin{aligned} Z &= \int_{\Theta} L(\theta) \pi(\theta) d\theta = \int_{\Theta} \int_0^\infty \mathbb{1}_{\{L(\theta) > \lambda\}}(\theta) d\lambda \pi(\theta) d\theta \\ &= \int_{\Theta} \int_0^\infty \mathbb{1}_{\{L(\theta) > \lambda\}}(\theta) \pi(\theta) d\lambda d\theta \\ &= \int_0^\infty \int_{\Theta} \mathbb{1}_{\{L(\theta) > \lambda\}}(\theta) \pi(\theta) d\theta d\lambda \end{aligned} \tag{1.3}$$

$$= \int_0^\infty \mu(\lambda) d\lambda \tag{1.4}$$

We may swap the integrals in step (1.3) thanks to Tonelli's theorem [16, p. 147]. With that, we have defined one of the key functions of Skilling's original paper [8]. $\mu : \mathbb{R} \rightarrow [0, 1]$ returns, for a given likelihood-threshold λ , the amount of prior mass which exists above that likelihood threshold:

$$\mu(\lambda) = \int_{\Theta} \mathbb{1}_{\{L(\theta) > \lambda\}}(\theta) \pi(\theta) d\theta = \int_{\{L(\theta) > \lambda\}} \pi(\theta) d\theta \tag{1.5}$$

It is a monotonically decreasing function with $\mu(0) = 1$ and $\lim_{\lambda \rightarrow \infty} \mu(\lambda) = 0$. A visualization is given in Figure 1.2.

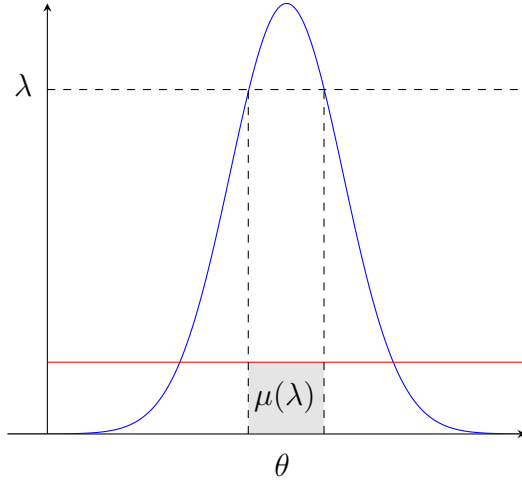


Figure 1.2: Visualization of the relationship between a likelihood threshold λ and the corresponding prior mass $\mu(\lambda)$ for a uniform prior (red) and a likelihood (blue).

We will reformulate the current version of the evidence integral, (1.4), a bit more:

$$\begin{aligned}
 Z &= \int_0^\infty \mu(\lambda) d\lambda \\
 &= \int_0^\infty \mu(\lambda) \cdot 1 d\lambda \\
 &\stackrel{\text{int. by parts}}{=} [\mu(\lambda)\lambda]_0^\infty - \int_0^\infty \mu'(\lambda)\lambda d\lambda \\
 &= \underbrace{\left(\lim_{\lambda \rightarrow \infty} \mu(\lambda)\lambda \right)}_{=0} - (\mu(0) \cdot 0) - \int_0^\infty \mu'(\lambda)\lambda d\lambda \tag{1.6}
 \end{aligned}$$

$$\begin{aligned}
 &= - \int_0^\infty \mu'(\lambda)\lambda d\lambda \\
 &\stackrel{\text{int. by sub.}}{=} - \int_1^0 \mu^{-1}(X) dX \tag{1.7} \\
 &= \int_0^1 \mu^{-1}(X) dX
 \end{aligned}$$

Note that $(\lim_{\lambda \rightarrow \infty} \mu(\lambda)\lambda) = 0$ in (1.6) because $\mu(\lambda)$ becomes 0 after some finite value for λ . The substitution used in (1.7) is $X = \mu(\lambda)$.

Following Skilling's notation, we denote the inverse of the prior mass function, μ^{-1} , by \mathcal{L} . This inverse exists because of μ 's monotonicity. It returns the corresponding

likelihood threshold $\mathcal{L}(X)$ to a given prior mass $X \in [0, 1]$.

$$Z = \int_0^1 \mu^{-1}(X) dX = \int_0^1 \mathcal{L}(X) dX \quad (1.8)$$

With that, we have accomplished our goal of formulating the evidence as a one dimensional integral. We integrate the likelihood-threshold function \mathcal{L} over the prior mass values X . The next section is about estimating this integral.

1.3.2 Sampling and Sorting

Imagine we had uniformly sampled n prior mass values $X_i \in [0, 1] \forall i \in \{1, \dots, n\}$. We could then use \mathcal{L} to compute their likelihood thresholds and sort them from lowest to highest. Since \mathcal{L} is a decreasing function, this would also sort the X_i in decreasing order of their own values. For simpler notation, the X_i 's sorting follows their indices. Imagine we had assigned them these indices after sorting.

$$\begin{array}{ccccccccc} \mathcal{L}(X_1) & < & \mathcal{L}(X_2) & < & \mathcal{L}(X_3) & < & \dots & < & \mathcal{L}(X_n) \\ X_1 & > & X_2 & > & X_3 & > & \dots & > & X_n \end{array} \quad (1.9)$$

In the case of there being two equal likelihood thresholds, we may randomly add a very small value to one of them to artificially create an order [8, p. 3].

As can be seen in Figure 1.3, we can approximate our target integral using the samples in the following Riemann sum [16, p. xvi]:

$$\begin{aligned} \int_0^1 \mathcal{L}(X) dX &\approx \sum_{i=1}^n \mathcal{L}(X_i) \cdot (X_{i-1} - X_i) \\ &\approx \sum_{i=1}^n \mathcal{L}(X_i) \cdot \Delta X_i \end{aligned} \quad (1.10)$$

where $\Delta X_i = X_{i-1} - X_i$ is called the prior mass shell of X_i , and we insert $X_0 = 1$. Sadly, we cannot actually compute $\mathcal{L}(X)$, so prior mass samples do not help us. We have to find another way of obtaining the terms that make up our evidence approximation in (1.10).

Instead of sampling prior masses directly, we may instead sample $\theta_1, \dots, \theta_n$ from the prior. We can prove that their corresponding prior masses are uniformly distributed.

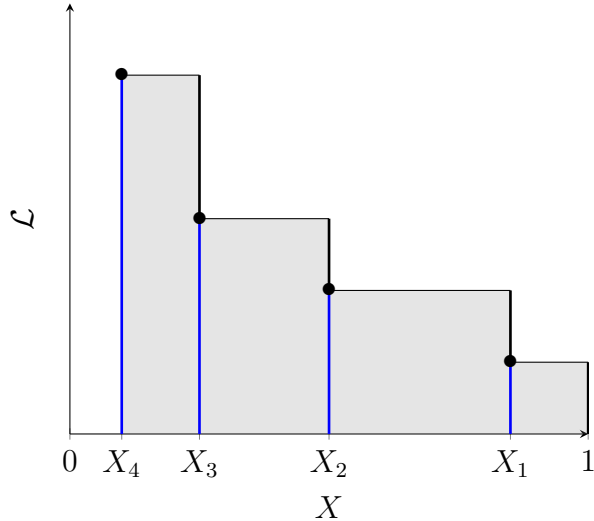


Figure 1.3: Visualization of how the evidence integral can be approximated using prior mass samples X_i sorted by their likelihoods, in this case using an upper sum. The shaded region is the approximate evidence. Based on a figure in [8, p. 4].

Proof: Prior Masses of Prior Samples are Uniformly Distributed

Let \mathbb{T} be a random variable representing samples from our prior. Its PDF is thus $f_{\mathbb{T}}(\theta) = \pi(\theta)$. Let $\mathbb{L} = L(\mathbb{T})$ and $\mathbb{M} = \mu(\mathbb{L})$ also be random variables. \mathbb{M} represents the prior masses. We want to prove that \mathbb{M} follows a uniform distribution. First, let us take a look at the distribution of the likelihoods \mathbb{L} . We can derive a nice formula for its PDF by starting with its definition as a marginal of the joint density of \mathbb{T} and \mathbb{L} :

$$\begin{aligned}
 f_{\mathbb{L}}(\lambda) &= \int_{\Theta} f_{\mathbb{L}, \mathbb{T}}(\lambda | \theta) d\theta \\
 &= \int_{\Theta} f_{\mathbb{L} | \mathbb{T}}(\lambda | \theta) f_{\mathbb{T}}(\theta) d\theta \\
 &= \int_{\Theta} f_{\mathbb{L} | \mathbb{T}}(\lambda | \theta) \pi(\theta) d\theta
 \end{aligned} \tag{1.11}$$

Because \mathbb{L} is a deterministic function of \mathbb{T} , the conditional density $f_{\mathbb{L} | \mathbb{T}}(\lambda | \theta)$ has to have $L(\theta)$ as the only possible outcome. This can be modeled using the Dirac delta function $\delta(x)$, which is defined to have the following property:

$$\int_{-\infty}^{\infty} f(x) \delta(x - y) dx = f(y), \tag{1.12}$$

and can informally be imagined as being zero everywhere except at $x = 0$, where it has an infinitely large spike [12, p. 600]. Modeling $f_{\mathbb{L}|\mathbb{T}}(\lambda | \theta) = \delta(\lambda - L(\theta))$, we can plug the result into (1.11):

$$f_{\mathbb{L}}(\lambda) = \int_{\Theta} \delta(\lambda - L(\theta)) \pi(\theta) d\theta,$$

and plug this representation of the PDF of \mathbb{L} into the formula for its cumulative distribution function (CDF):

$$\begin{aligned} F_{\mathbb{L}}(\lambda) &= \int_0^{\lambda} f_{\mathbb{L}}(\lambda') d\lambda' \\ &= \int_0^{\lambda} \int_{\Theta} \pi(\theta) \delta(\lambda' - L(\theta)) d\theta d\lambda' \\ &= \int_{\Theta} \int_0^{\lambda} \pi(\theta) \delta(\lambda' - L(\theta)) d\lambda' d\theta \end{aligned} \tag{1.13}$$

$$\begin{aligned} &= \int_{\Theta} \pi(\theta) \int_0^{\lambda} \delta(\lambda' - L(\theta)) d\lambda' d\theta \\ &= \int_{\Theta} \pi(\theta) \mathbb{1}_{\{L(\theta) < \lambda\}}(\theta) d\theta \end{aligned} \tag{1.14}$$

$$\begin{aligned} &= \int_{\{L(\theta) < \lambda\}} \pi(\theta) d\theta \\ &= 1 - \mu(\lambda) \end{aligned} \tag{1.15}$$

In step (1.13), we again use Tonelli's theorem to swap the order of the integrals [16, p. 147]. Step (1.14) uses the main property of the Dirac delta function from (1.12). The integral is 1 as long as the spike of the delta function (which is in this case shifted to be at $L(\theta)$) is inside the integral's bounds. Lastly, in step (1.15) we recognize the definition of μ from (1.5), only with a flipped inequality sign in the super level set.

The probability integral transform tells us that a random variable $\mathbb{Y} = f(\mathbb{X})$ is uniform if f is the CDF of \mathbb{X} [17, p. 54]. This, combined with (1.15) means that a random variable $\bar{\mathbb{M}} = 1 - \mu(\mathbb{L})$ would be uniformly distributed, since $1 - \mu(\lambda)$ is the CDF of \mathbb{L} . Finally, since \mathbb{M} 's values are simply the values of $\bar{\mathbb{M}}$ mirrored at $m = 0.5$, \mathbb{M} is also uniformly distributed. \square

With that, we have the first part we need to approximate the evidence using (1.10):

the likelihood thresholds of prior mass samples. This leaves the prior mass samples themselves. We cannot compute the prior masses of our samples $\theta_1, \dots, \theta_n$, but we are able to estimate them using order statistics.

Order statistics study the distributions of random values when they are sorted. The i -th order statistic represents the distribution of the i -th lowest value in a set of n randomly drawn values. We make use of the fact that when n values are drawn from a Uniform(0, 1) distribution, the i -th order statistic follows a Beta($i, n - i + 1$) distribution [18, p. 63]. As we remember from (1.9), we can indirectly order our samples' prior masses if we order them by their likelihoods. We know that the sample with the i -th lowest likelihood value will also have the i -th highest, or equally the $(n - i + 1)$ -th lowest, prior mass. The prior mass thus follows a Beta($n - i + 1, i$) distribution, and we can estimate it by either sampling from the distribution or by using its mean.

In θ_i , we have thus obtained a likelihood value $L(\theta_i)$ and an estimate for its prior mass $X_i \sim \text{Beta}(n - i + 1, i)$. We could now simply sample n values from the prior, compute their likelihoods and estimate their prior masses to get an estimate of the evidence according to (1.10). This would generally, however, lead to horribly inaccurate estimates. Because the area of the sample space with high likelihood values is generally very small and away from the high prior values (where the prior samples will concentrate), finding samples with high likelihood that contribute significantly to the evidence would be difficult [8, p. 7]. The next section shows how this problem is solved in Nested Sampling.

1.3.3 Introducing a Likelihood Constraint

Nested Sampling generates contributions to the evidence as in (1.10) iteratively. This allows us to modify how the contributions are sampled as the algorithm goes along. Specifically, we can introduce a constraint that forces new contributions to be sampled in regions of higher likelihood. This solves the problem of prior samples missing the regions with significant posterior mass.

We need an ensemble of prior samples to use our strategy for estimating prior masses from the last section, so we start by drawing n prior samples $\theta_1, \dots, \theta_n$, which we call the live points. Then we take the sample with the lowest likelihood, θ_{\min} remove it from the live points and save it as a dead point. We also use it to compute the first contribution to the evidence as in (1.10), which is the product of its likelihood and an estimate of its prior mass shell. Because θ_{\min} has the smallest likelihood of all live points, it will also have the largest associated prior mass, X_1 . This lets us simplify

the estimate of its prior mass shell:

$$\Delta X_1 = X_0 - X_1 = 1 - X_1$$

X_1 follows a Beta($n, 1$) distribution and, one of the properties of the Beta distribution is that if $\mathbb{X} = 1 - \mathbb{Y}$ and $\mathbb{Y} \sim \text{Beta}(a, b)$, then $\mathbb{X} \sim \text{Beta}(b, a)$ [19, p. 5.17.2.]. So ΔX_1 follows a Beta($1, n$) distribution, and we can again estimate it either by sampling or by using the mean.

The likelihood of θ_{\min} becomes the likelihood constraint L^* , meaning all points we sample thereafter have to have a likelihood higher than it. Luckily, all other live points already fulfill this constraint, since we chose the one with the lowest likelihood to remove. This means we only have to draw one new live point according to the constraint, $\theta_{\text{new}} \sim \pi(\theta) \mathbb{1}_{\{L(\theta) > L^*\}}(\theta)$. We call this step likelihood-restricted prior sampling (LRPS). Having sampled a new live point, we again take the sample with the lowest likelihood, remove it from the live points, add its contribution to the evidence and set its likelihood as the new likelihood constraint, etc.

To be sure that this strategy is correct, we have to show that the prior masses of these samples from the likelihood-restricted prior are still uniformly distributed; a proof of this can be found in the Appendix. Also, the prior masses of $\theta_1, \dots, \theta_n$ cannot follow a Beta($i, n - i + 1$) distribution anymore, since the prior masses are now distributed uniformly on $[0, \mu(L^*)]$ instead of $[0, 1]$. However, if we call $\mu(L^*)$ the remaining prior mass, then the fraction of this mass that each drawn sample is connected to, $\frac{\mu(L(\theta))}{\mu(L^*)}$, is still uniformly distributed on $[0, 1]$. So we can get our estimate of the prior mass shell of the lowest-likelihood sample by sampling a mass fraction $f \sim \text{Beta}(1, n)$ and multiplying it by the remaining prior mass $\mu(L^*)$.

As the likelihood constraint increases, the LRPS-samples will come from regions of higher and higher likelihood. This process is carried out for a given number of iterations or, more sophisticatedly, until an estimate of the remaining evidence in relation to the accumulated evidence becomes smaller than some chosen ϵ . A simple estimate of an upper bound of the remaining evidence can be made by taking the highest likelihood present in the live points and multiplying it by the remaining prior mass. Over the course of the algorithm, the evidence is computed according to (1.10), by multiplying each dead point's likelihood and estimated prior mass shell and summing over all of them.

Posterior samples can also be generated easily. One randomly draws from the dead points, where each dead point's probability to be sampled is proportional to the

product of its likelihood and its corresponding prior mass shell [20, p. 9].

Inputs to the algorithm are the prior and likelihood functions as well as the stopping threshold (or number of iterations) and the number of live points. The stopping threshold determines how much of the evidence to accumulate, while the number of live points works like a resolution parameter. The more live points we keep, the more likely we are to find and explore small peaks in the likelihood, making the evidence estimate more accurate. More live points also cause the algorithm to take longer, since each evidence contribution will be associated with a smaller prior mass. The number of iterations required to fulfill the same stopping threshold scales linearly with the number of live points. Specifically, the run time of nested sampling can be described as $T \sim T_L \cdot n_{\text{live}} \cdot f_{\text{sampler}} \cdot \mathcal{D}_{\text{KL}}$ [20, p. 1], where

- T_L is the time required to evaluate the likelihood once,
- n_{live} is the number of live points,
- T_{LRPS} is the mean time required for the LRPS step over the course of the run,
- and \mathcal{D}_{KL} is the Kullback-Leibler Divergence [21, p. 6] between prior and posterior.

See Algorithm 1 for an overview of the Nested Sampling procedure and see a visualization in Figure 1.4.

Having explained the main ideas of Nested Sampling, let us now get into the details of the most computationally intensive and least clearly defined step of it, LRPS.

Algorithm 1 NestedSampling (n, ϵ, π, L)

```

sample  $\theta_1, \dots, \theta_n$  from the prior  $\pi$ 
 $live\_points \leftarrow [\theta_1, \dots, \theta_n]$ 
 $mass \leftarrow 1$ 
 $dead\_points \leftarrow []$ 
 $Z \leftarrow 0$ 
repeat
     $L_{\min} \leftarrow \min_{\theta \in live\_points} L(\theta)$ 
     $\theta_{\min} \leftarrow \operatorname{argmin}_{\theta \in live\_points} L(\theta)$ 
    remove  $\theta_{\min}$  from  $live\_points$ 
    append  $\theta_{\min}$  to  $dead\_points$ 
    sample  $f$  from Beta(1,  $n$ )
     $mass\_shell \leftarrow mass \cdot f$ 
     $mass \leftarrow mass - mass\_shell$ 
     $Z \leftarrow Z + mass\_shell \cdot L_{\min}$ 
    sample  $\theta_{\text{new}}$  from likelihood-restricted prior  $\pi(\theta) \mathbb{1}_{\{L(\theta) > L^*\}}$ 
    append  $\theta_{\text{new}}$  to  $live\_points$ 
     $L_{\max} \leftarrow \max_{\theta \in live\_points} L(\theta)$ 
until  $(mass \cdot L_{\max})/Z < \epsilon$ 
return  $Z, dead\_points$ 

```

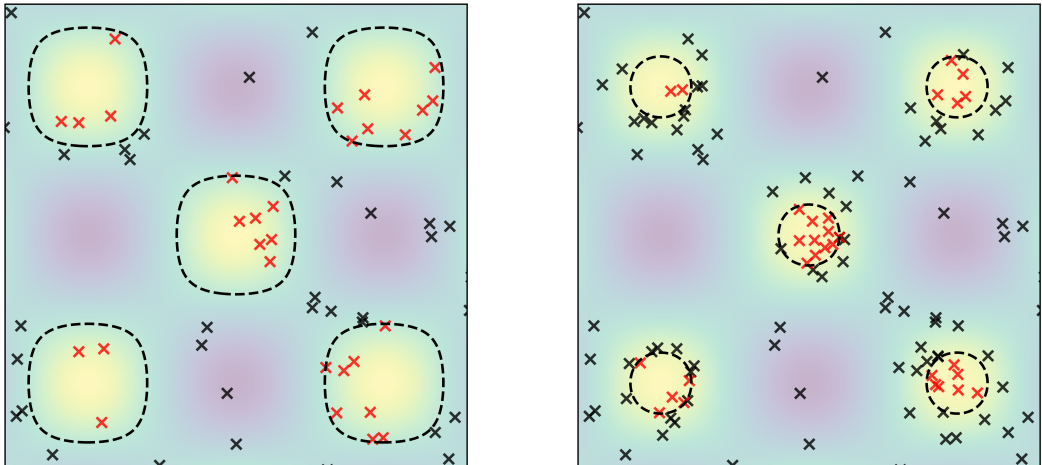


Figure 1.4: Intermediate states of a Nested Sampling run on an eggcrate-shaped likelihood with a uniform prior. Black crosses are all dead points up to this point, red crosses are live points. All live points are inside the current likelihood constraint contour. The likelihood is visualized by the colored background, lighter colors represent higher likelihood values. The left image shows an earlier iteration than the right one, as can be seen by the lower number of dead points and the looser likelihood constraint contours.

1.4 Likelihood-Restricted Prior Sampling

In the sampling of new points from the likelihood-restricted prior lies most of the computational work of Nested Sampling. The original paper by Skilling provides little guidance for this step, only that "such points will usually be found by some MCMC approximation, ..." [8, p. 6] In this section, we summarize multiple ways to do LRPS while presenting their advantages and drawbacks, working our way up from the simplest methods to more complex ones.

1.4.1 Rejection Sampling

Rejection Sampling is the simplest way to sample from the constrained prior. We generate a sample from the prior, compute its likelihood and check if it satisfies the likelihood constraint. If it does, we accept the sample; otherwise, we reject it.

Rejection Sampling is infeasible for larger models due to it being terribly inefficient in higher dimensions. The acceptance rate of the generated samples is proportional to how much of the prior mass is inside the likelihood constraint. Since the prior mass inside the likelihood constraint is expected to shrink by a factor of $\frac{1}{1+n}$ (mean of the Beta($1, n$) distribution) in each iteration, the acceptance rate quickly plummets, leading to most proposals being rejected.

1.4.2 Discretized LRPS

Another simple, non-MCMC method for LRPS involves discretizing the sample space into a uniform grid. In each iteration, we randomly draw one of the grid points with likelihood higher than the constraint, with the probability of each point being drawn being proportional to its prior.

Like Rejection Sampling, this method falls short because of its lacking performance and can only be used for models with few parameters and priors with finite support. Since the number of grid points scales exponentially with the dimensionality of the sample space, this method is hopelessly time- and memory-inefficient for problems with even a modest number of dimensions.

1.4.3 Metropolis Algorithm

The Metropolis algorithm, already sketched out in Section 1.1, is an MCMC method generating dependent samples using a proposal distribution. The proposal distribution, often a normal distribution, creates a proposal θ_p based on the last sample

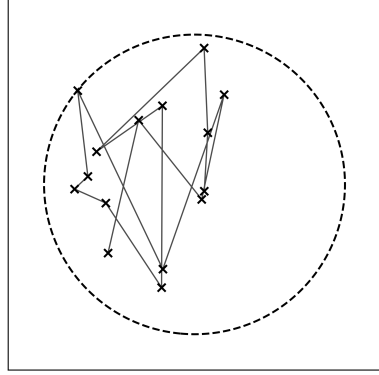


Figure 1.5: Visualization of the Metropolis algorithm in a two-dimensional sample space. The dashed line indicates the likelihood constraint boundary, the dot is the starting point and each cross is a sampled point.

θ . This proposal is then accepted with a probability $\min\left(\frac{P(\theta_p)}{P(\theta)}, 1\right)$. In LRPS, this process is repeated a given number of times to decorrelate the samples. The more intermediate samples are drawn, the less the first and last sample correlate. Proposals which do not satisfy the likelihood constraint are never accepted. Details can be seen in Algorithm 2. If the proposal distribution is not symmetric, the standard Metropolis algorithm fails, but a variant called Metropolis-Hastings can be used [12, p. 365f.].

Algorithm 2 LRPSMetropolis ($n, \theta_0, \pi, \sigma, L, L^*$)

```

 $\theta \leftarrow \theta_0$ 
for  $n$  iterations do
    sample  $\theta_p$  from  $\mathcal{N}(\theta, \sigma^2)$ 
    sample  $u$  from Uniform(0, 1)
    if  $L(\theta_p) > L^*$  and  $\pi(\theta_p)/\pi(\theta) > u$  then
         $\theta \leftarrow \theta_p$ 
    end if
end for
return  $\theta$ 

```

The main advantage of the Metropolis algorithm in LRPS is its local exploration. Since it always starts from a valid point and explores its local surroundings, its acceptance rate can be much higher than that of Rejection Sampling. It does, however, have two major disadvantages. Firstly, because the samples are dependent, we have to draw many intermediate samples before returning an actual sample, to allow them to decorrelate. Secondly, since the proportion of prior space within the

likelihood constraint becomes smaller with each Nested Sampling iteration, the step size (standard deviation of the proposal distribution) required to efficiently explore the space changes continually. This second problem can be overcome by using an adaptive step size. A simple approach is to decrease the step size by some factor each time a sample lands outside the likelihood constraint while increasing it whenever a sample lands inside it. More nuanced methods for step size adaptation have been developed as well [22], but will not be covered in this thesis.

1.4.4 Hamiltonian Monte Carlo

Hamiltonian Monte Carlo (HMC) [3] is a widely used MCMC algorithm for Bayesian model fitting. Normally used to sample from the posterior of a Bayesian model all on its own, we can also appropriate it for LRPS. As the theory behind HMC is quite involved, I will only give an overview of the algorithm, not delving into the reasons for why it works.

As HMC is an MCMC method, it generates dependent samples like the Metropolis algorithm does. However, it uses a physical analogy to find samples that are much further away from the starting point, thus decorrelating and exploring the target distribution faster.

The negative logarithm of the target distribution is interpreted as potential energy. One can imagine this as a hills-and-valleys landscape. Each sample is viewed as a movable particle in this space. Starting with a sample, a random, normally distributed vector is drawn. This vector represents a momentum that the sample particle has. The path of the particle across the landscape with its given starting momentum is then simulated using a special type of solver for the ordinary differential equations describing the dynamics of the particles which is called a symplectic integrator. At an arbitrarily chosen point of time, the particle is stopped. The resulting position of the sample is then treated like a Metropolis proposal and accepted with probability based on the ratio of probability values of the proposal and the last sample. A visualization of this process can be seen in Figure 1.6. Betancourt [23] provides a thorough explanation of HMC with solid theoretical foundations.

HMC can be adapted for LRPS. In this case, the negative logarithm of the prior provides the landscape for the particles to move around in. The starting spot for a particle is always chosen to satisfy the likelihood constraint (e.g. by choosing one of the live points). HMC evolves the particle through the prior space to generate a new sample. The main adaptation for LRPS concerns what happens when the particle crosses the likelihood constraint boundary. In this case, it is reflected off the

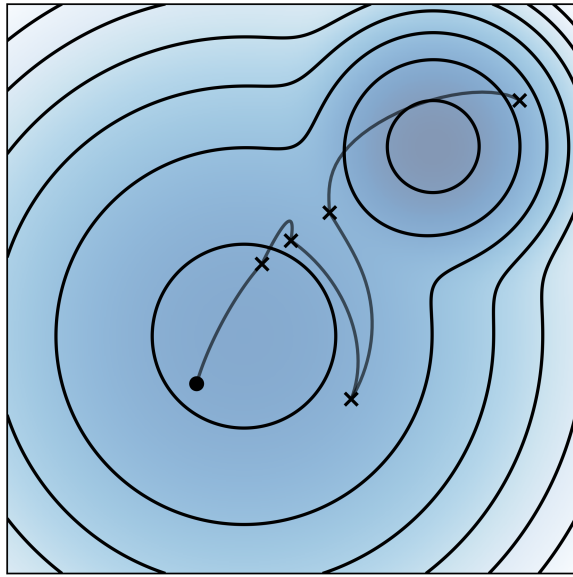


Figure 1.6: Visualization of HMC in a two-dimensional sample space. Contour lines and shading indicate the negative log probability of the target distribution (a mixture of two Gaussians). The dot is the starting point and each cross is a sampled point.

boundary to stay inside the valid region. This version of HMC was introduced by Betancourt in [9].

Like the Metropolis Algorithm, HMC for LRPS requires an adaptive step size. Without it, because the valid region to sample from becomes arbitrarily small, Nested Sampling would reach a likelihood level at which the step size is so large that HMC has to reflect with every integration step. This causes problems since the likelihood gradient used for reflection is calculated at the end of the integration step that lands outside the likelihood constraint. If the step size is very large in relation to the valid sampling area, the gradient will be calculated far away from the actual constraint boundary, leading to inaccurate reflection and biased sampling. See the visualization in Figure 1.7.

Having introduced Nested Sampling, we require one more piece of background knowledge before we are ready to tackle the contributions of this thesis.

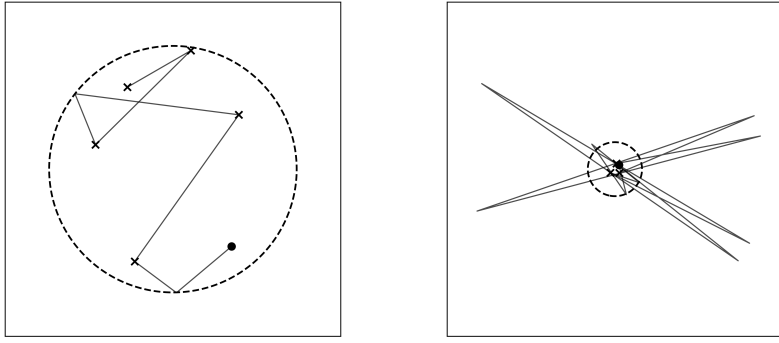


Figure 1.7: Left: An iteration of HMC for LRPS with reflection consisting of five samples on a standard-normal-likelihood-restricted uniform prior space. The black dot is the starting spot, each cross is a generated sample. Right: A later iteration of the same example. Note how every integration step contains a reflection and how far away the reflection points are from the actual boundary.

1.5 The Barrier Method

This section provides an introduction to the Barrier Method [24, p. 568], an algorithm for solving constrained convex optimization problems. We will later incorporate ideas of this method into Nested Sampling.

The Barrier Method is used to solve optimization problems of the form

$$\begin{aligned} & \text{minimize} && f(x) \\ & \text{subject to} && f_i(x) \leq 0 \quad \text{for } i = 1, \dots, m \end{aligned} \tag{1.16}$$

with f and all f_i being convex and twice continuously differentiable. The problem also has to be strictly feasible, meaning that there exists an \tilde{x} in the domain of f , such that $f_i(\tilde{x}) < 0 \forall i \in \{1, \dots, m\}$ [24, p. 561].

We reformulate the optimization problem from (1.16) to be unconstrained by incorporating the constraints into the objective function

$$\text{minimize} \quad f(x) + \sum_{i=1}^m I(f_i(x)) \tag{1.17}$$

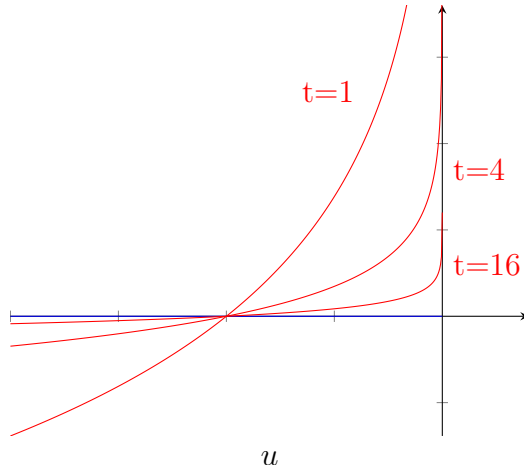


Figure 1.8: Visualization of the exact barrier function I in blue, and three log barrier functions (with $t = 1, 4, 16$) in red. The log barrier becomes a better approximation as t increases.

with $I(u)$ being defined as follows:

$$I(u) = \begin{cases} 0, & \text{if } u \leq 0 \\ \infty, & \text{if } u > 0 \end{cases} \quad (1.18)$$

By applying an infinitely large penalty to infeasible points, (1.17) accurately represents the original problem. However, because the added terms are not differentiable, we would no longer be able to use gradient information to solve this formulation of the problem. This is a problem because gradients are key to solving optimization problems. In particular, the most fundamental solver, Newton's Method, requires that the objective function is differentiable [24, p. 563].

To circumvent this shortcoming, we approximate I using the differentiable log barrier function:

$$\hat{I}(u) = -\frac{1}{t} \log(-u) \quad (1.19)$$

t is a parameter of the function, with larger t leading to better approximations. This behavior can be seen in Figure 1.8. It should be noted that \hat{I} is only defined for feasible points [24, p. 563].

The new, approximate optimization problem is:

$$\text{minimize} \quad f(x) + \sum_{i=1}^m -\frac{1}{t} \log(-f_i(x)) \quad (1.20)$$

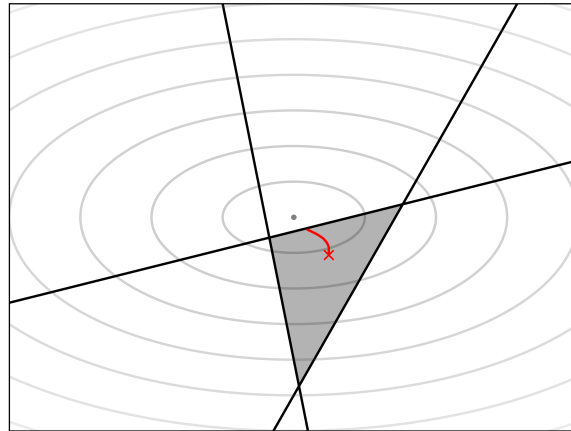


Figure 1.9: Central path of an example optimization problem. The shaded area is the feasible region, given by the constraint functions in black. The gray lines indicate contours of the objective function, with the unconstrained optimum at the gray dot. The central path of the problem is shown in red. $x^*(1)$ is marked by a red cross.

We can multiply the objective function by t to obtain:

$$\text{minimize} \quad t \cdot f(x) + \sum_{i=1}^m -\log(-f_i(x)) \quad (1.21)$$

By varying the parameter t , we obtain different problems with different solutions. We will refer to the solution of (1.21) for a certain value of t as $x^*(t)$. The set of solutions for all possible values of t , $\{x^*(t) \mid t > 0\}$, is called the central path of the problem. It converges to the true solution as $t \rightarrow \infty$, as can be seen in Figure 1.9 [24, p. 564].

Solving the problem in (1.21) for a large value of t provides a good estimation of the exact solution. $x^*(t)$ is provably $\frac{m}{t}$ -suboptimal, meaning that its objective function value is at most $\frac{m}{t}$ greater than the optimal value [24, p. 566].

However, as the log barrier function becomes a better approximation of the strict barrier with larger t , its derivatives become more extreme. This causes the standard optimization procedures, such as Newton's method, to fail [24, p. 564]. The Barrier Method is an approach that solves this issue by applying an iterative strategy. In each iteration, $x^*(t_i)$ is computed using Newton's Method in what's called a centering step. The value of t_i increases with each iteration, and the result of the previous iteration is used as the starting point for the current one. This stabilizes the centering

steps [24, p. 569]. See Algorithm 3.

Algorithm 3 BarrierMethod (x_0, t_0, μ, ϵ)

```
 $x \leftarrow x_0$ 
 $t \leftarrow t_0$ 
repeat
    compute  $x^*(t)$  by minimizing  $t \cdot f(x) + \sum_{i=1}^m -\log(-f_i(x))$  starting at  $x$ 
     $x \leftarrow x^*(t)$ 
     $\hat{\epsilon} \leftarrow \frac{m}{t}$ 
     $t \leftarrow \mu t$ 
until  $\hat{\epsilon} < \epsilon$ 
return  $x$ 
```

The most important idea we borrow from the Barrier Method is how the log barrier function provides a way to make a hard boundary soft and differentiable. In the next chapter, we incorporate this idea into the LRPS step of Nested Sampling.

2 Nested Sampling with Barriers

2.1 Motivation

As was shown in Section 1.4, LRPS is difficult. Because the likelihood constraint grows tighter and the ratio of the valid area to the area of the whole sample space decreases steadily, finding samples within the constraint boundary becomes more difficult with every Nested Sampling iteration. For methods like Rejection Sampling and the Metropolis algorithm, this manifests in low acceptance rates of proposals, which lead to wasted computational work, or (if an adaptive step size is used) in highly correlated samples. For HMC adapted to LRPS, detecting the point at which the particle breaches the likelihood constraint boundary and must be reflected also becomes harder, since the distance the particle can travel before leaving the valid region decreases with each iteration. All these methods only notice the likelihood constraint boundary once they have crossed it. The proposals for Rejection Sampling and the Metropolis Algorithm do not take into account the likelihood at all, having to reject (intermediate) samples that cross the boundary, and while HMC for LRPS can reflect during proposal generation, this only happens after the boundary has been crossed. We would like an approach that softens the hard likelihood constraint and pushes the samples away from the boundary during sampling.

Thinking back to the Barrier Method from Section 1.5, we can make the following observation: The log barrier also softens a hard constraint function and allows the optimization algorithm to feel the constraint before crossing it. This leads us to the main idea of this thesis: incorporating the log barrier from the Barrier Method into the LRPS step of Nested Sampling.

2.2 Derivation

2.2.1 Deriving the Log Barrier Term

In this section we draw parallels between LRPS and convex optimization to find a way to use log barriers in a probabilistic setting.

Convex optimization is concerned with minimizing a function constrained by a set of convex functions (as can be seen in (1.16)). In LRPS, we sample from a probability distribution $\pi(\theta)$, constrained by $L(\theta) > L^*$. Even though this constraint is not necessarily convex (for most real-world applications it will not be), it still constricts the space we are working on and thus takes on a similar role to the constraint functions in convex optimization. In the following paragraphs, we will pretend that LRPS is an optimization problem with $\pi(\theta)$ as the objective function and $L(\theta) > L^*$ as the constraint. This is done to apply the idea of the log barrier from Section 1.5 to LRPS, which will lead us to an important term that softens the likelihood constraint boundary. That said, we are only doing this for inspiration. We will not actually be solving the optimization problem we set up:

$$\text{maximize } \pi(\theta) \quad \text{subject to } L(\theta) > L^*$$

Optimization problems over probabilities are usually solved in logarithmic space rather than probability space for reasons like easier differentiation and numerical stability. We do the same, taking the logarithm of both the objective function and both sides of the likelihood constraint. This does not change the solution of the optimization problem because the logarithm is a monotonic function and thus preserves order in both the objective function and the constraint. We also multiply the objective function by -1 so we can minimize instead of maximizing, to match the optimization problems from Section 1.5:

$$\begin{aligned} & \text{maximize } \pi(\theta) && \text{subject to } L(\theta) > L^* \\ \iff & \text{minimize } -\log(\pi(\theta)) && \text{subject to } L(\theta) > L^* \\ \iff & \text{minimize } -\log(\pi(\theta)) && \text{subject to } \log(L(\theta)) > \log(L^*) \\ \iff & \text{minimize } -\log(\pi(\theta)) && \text{subject to } l(\theta) > l^* \\ \iff & \text{minimize } -\log(\pi(\theta)) && \text{subject to } l^* - l(\theta) < 0 \end{aligned}$$

We use the exact barrier function from (1.18) to incorporate the constraints into the

objective function:

$$\text{minimize} \quad -\log(\pi(\theta)) + I(l^* - l(\theta))$$

Next, we generate the associated approximate problem using log barriers (see (1.19) and (1.20)):

$$\begin{aligned} & \text{minimize} \quad -\log(\pi(\theta)) + \hat{I}(l^* - l(\theta)) \\ \iff & \text{minimize} \quad -\log(\pi(\theta)) - \frac{1}{t} \log(l(\theta) - l^*) \end{aligned}$$

Then we negate and exponentiate the objective function to return to a maximization problem in probability space:

$$\begin{aligned} & \text{minimize} \quad -\log(\pi(\theta)) - \frac{1}{t} \log(l(\theta) - l^*) \\ \iff & \text{maximize} \quad \exp\left(-\left(-\log(\pi(\theta)) - \frac{1}{t} \log(l(\theta) - l^*)\right)\right) \\ \iff & \text{maximize} \quad \pi(\theta) (l(\theta) - l^*)^{\frac{1}{t}} \end{aligned} \tag{2.1}$$

We obtain a term that will be important for the rest of this thesis, the log barrier term:

$$(l(\theta) - l^*)^{\frac{1}{t}} \tag{2.2}$$

For valid θ , the log barrier term decreases as the (log-)likelihood of θ approaches the minimum (log-)likelihood. When used as a factor to the prior as in (2.1), this discourages the sampling of θ closer to the likelihood constraint boundary, effectively letting the sampler feel the boundary before crossing it. In the next section we integrate this term into Nested Sampling.

2.2.2 Incorporating the Log Barrier Term

Having derived a term that represents a log barrier in probability space, we are now looking for a way to use it during LRPS without introducing a bias into our sampler.

To this end, we expand the sampling space by adding a one-dimensional real variable q , taking values in (q_{\min}, q_{\max}) :

$$\theta \rightarrow (\theta, q)$$

Because we have full control over how q is distributed, we can design it so that it affects the sampling of θ in just the way we want. First, we define q to be independent

of θ :

$$P(\theta, q) = P(\theta) P(q)$$

By applying Bayes' rule to the marginal distributions of θ and q , we can see that the independence follows through to the likelihood:

$$\begin{aligned} P(\theta, q | D) &= P(\theta | D) P(q | D) \\ &= \frac{P(D | \theta) P(\theta)}{\int_{\Theta} P(D | \theta) P(\theta) d\theta} \frac{P(D | q) P(q)}{\int_Q P(D | q) P(q) dq} \\ &= \frac{P(D | \theta) P(\theta) P(D | q) P(q)}{\int_{\Theta} P(D | \theta) P(\theta) d\theta \int_Q P(D | q) P(q) dq} \\ &= \frac{P(D | \theta) P(D | q) P(\theta) P(q)}{\int_{\Theta} P(D | \theta) P(\theta) d\theta \int_Q P(D | q) P(q) dq} \\ &= \frac{L_{\theta}(\theta) L_q(q) \pi_{\theta}(\theta) \pi_q(q)}{Z_{\theta} Z_q} \\ &= \frac{L(\theta, q) \pi(\theta, q)}{Z_{\theta, q}} \end{aligned} \tag{2.3}$$

In (2.3), we recognize Bayes' rule on the combined space (θ, q) and define $L(\theta, q) = L_{\theta}(\theta) L_q(q)$, $\pi(\theta, q) = \pi_{\theta}(\theta) \pi_q(q)$ and $Z_{\theta, q} = Z_{\theta} Z_q$ accordingly. This lets us freely choose the likelihood and prior of our new variable q . It also shows that we can perform Nested Sampling on the (θ, q) -space and recover the original evidence as $Z_{\theta} = \frac{Z_{\theta, q}}{Z_q}$.

Now, let us take a look at LRPS on this expanded space. We will call the likelihood-restricted prior $\bar{\pi}$:

$$(\theta, q) \sim \bar{\pi}(\theta, q | L^*)$$

$$\bar{\pi}(\theta, q | L^*) = \pi(\theta, q) \mathbb{1}_{\{L(\theta, q) > L^*\}}$$

We employ a technique called collapsed Gibbs sampling [25] to sample from the likelihood-restricted prior. By first sampling from the marginal distribution of θ , we can then use the obtained value to sample from the conditional distribution of q :

$$\theta \sim \bar{\pi}(\theta | L^*)$$

$$q \sim \bar{\pi}(q | L^*, \theta)$$

By defining the likelihood of q as $L_q(q) = \frac{1}{q}$, we can reshape the likelihood-restricted priors:

$$\begin{aligned}
\bar{\pi}(\theta | L^*) &= \int_{q_{\min}}^{q_{\max}} \bar{\pi}(\theta, q | L^*) dq \\
&= \int_{q_{\min}}^{q_{\max}} \pi_\theta(\theta) \pi_q(q) \mathbb{1}_{\{L(\theta, q) > L^*\}}(\theta, q) dq \\
&= \pi_\theta(\theta) \int_{q_{\min}}^{q_{\max}} \pi_q(q) \mathbb{1}_{\{L_\theta(\theta) L_q(q) > L^*\}}(\theta, q) dq \\
&= \pi_\theta(\theta) \int_{q_{\min}}^{q_{\max}} \pi_q(q) \mathbb{1}_{\{L_\theta(\theta)/q > L^*\}}(\theta, q) dq \\
&= \pi_\theta(\theta) \int_{q_{\min}}^{q_{\max}} \pi_q(q) \mathbb{1}_{\{q < L_\theta(\theta)/L^*\}}(\theta, q) dq \\
&= \pi_\theta(\theta) \int_{q_{\min}}^{L^*/L_\theta(\theta)} \pi_q(q) dq \\
&= \pi_\theta(\theta) \Pi_q(L_\theta(\theta)/L^*)
\end{aligned}$$

$$\bar{\pi}(q | L^*, \theta) = \pi_q(q) \mathbb{1}_{\{q < L_\theta(\theta)/L^*\}}$$

Where Π_q is the antiderivative of π_q , i.e. the CDF of q . Since we are free to define Π_q however we want, we can use it to insert the log barrier term from (2.2):

$$\begin{aligned}
\Pi_q(L_\theta(\theta)/L^*) &\stackrel{!}{=} (l_\theta(\theta) - l^*)^{\frac{1}{t}} \\
\Pi_q(L_\theta(\theta)/L^*) &= (\log(L_\theta(\theta)) - \log(L^*))^{\frac{1}{t}} \\
\Pi_q(L_\theta(\theta)/L^*) &= \log(L_\theta(\theta)/L^*)^{\frac{1}{t}} \\
\text{let } q &= L_\theta(\theta)/L^* \\
\Pi_q(q) &= \log(q)^{\frac{1}{t}}
\end{aligned} \tag{2.4}$$

With this, we have defined the shape of the CDF of q in such a way that the log barrier term appears in LRPS. In (2.4), we implicitly define $q_{\max} = 1$, since $L_\theta(\theta)$ always has to be larger than L^* to satisfy the likelihood constraint. However, as can be seen in Figure 2.1, the CDF of q is unnormalized unless we choose $q_{\max} = e$.

We can normalize it for any other q_{\max} by scaling Π_q to have a value of 1 at $q = q_{\max}$.

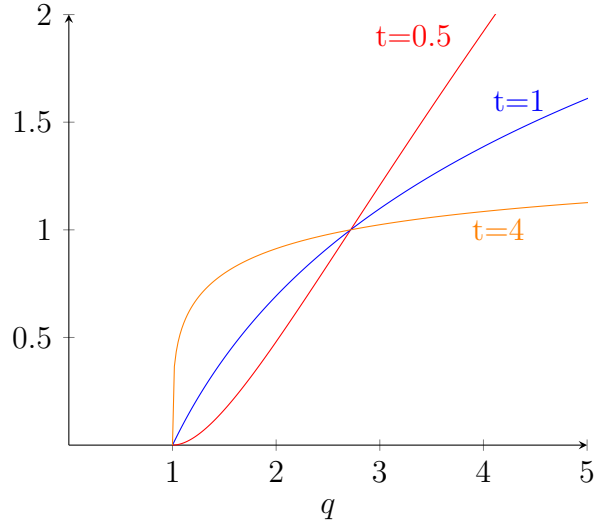


Figure 2.1: Visualization of the unnormalized CDF Π_q of q for different values of t and $q_{\max} = 5$.

We called the normalized version $\hat{\Pi}_q$:

$$\hat{\Pi}_q(q) = \frac{\Pi_q(q)}{\Pi_q(q_{\max})} \quad \text{if } q \in (1, q_{\max})$$

In all, we define the CDF for q as follows:

$$\hat{\Pi}_q(q) = \begin{cases} 0 & \text{if } q \leq 1 \\ \frac{\log(q)^{\frac{1}{t}}}{\log(q_{\max})^{\frac{1}{t}}} & \text{if } q \in (1, q_{\max}) \\ 1 & \text{if } q \geq q_{\max} \end{cases}$$

Differentiating $\hat{\Pi}_q$ gives us the PDF of q :

$$\frac{d\Pi_q}{dq}(q) = \pi_q(q) = \begin{cases} 0 & \text{if } q \leq 1 \\ \frac{\log(q)^{\frac{1}{t}-1}}{tq \log(q_{\max})^{\frac{1}{t}}} & \text{if } q \in (1, q_{\max}) \\ 0 & \text{if } q \geq q_{\max} \end{cases}$$

With that, we have defined both the likelihood and the prior of q in a way that incorporates the log barrier term into LRPS. This lets us write down the modified version of Nested Sampling in Algorithm 4. The changes from the original are the following:

1. For each starting θ , also sample a q .

2. Use the joint likelihoods of θ and q , $L(\theta, q) = \frac{L_\theta(\theta)}{q}$, instead of just the likelihood of θ .
3. Sample θ_{new} from the modified constrained prior $\pi_\theta(\theta) \Pi_q(l_\theta(\theta) - l^*)$.
4. Sample q_{new} from the constrained prior $\pi_q(q) \mathbb{1}_{\{q < L_\theta(\theta_{\text{new}})/L^*\}}$ dependent on the sampled θ_{new} .
5. Divide out $Z_q(t, q_{\max})$ from the evidence before returning it.

Algorithm 4 NestedBarrierSampling ($n, \epsilon, \pi_\theta, L_\theta, t, q_{\max}$)

```

sample  $\theta_1 \dots \theta_n$  from the prior  $\pi_\theta$ 
sample  $q_1 \dots q_n$  from the prior  $\pi_q$ 
 $live\_points \leftarrow [(\theta_1, q_1) \dots (\theta_n, q_n)]$ 
 $mass \leftarrow 1$ 
 $dead\_points \leftarrow []$ 
 $Z \leftarrow 0$ 
repeat
   $L_{\min} \leftarrow \min_{(\theta, q) \in live\_points} L(\theta, q)$ 
   $(\theta_{\min}, q_{\min}) \leftarrow \operatorname{argmin}_{(\theta, q) \in live\_points} L(\theta, q)$ 
  remove  $(\theta_{\min}, q_{\min})$  from  $live\_points$ 
  append  $\theta_{\min}$  to  $dead\_points$ 
  sample  $f$  from Beta(1,  $n$ )
   $mass\_shell \leftarrow mass \cdot f$ 
   $mass \leftarrow mass - mass\_shell$ 
   $Z \leftarrow Z + mass\_shell \cdot L_{\min}$ 
  sample  $\theta_{\text{new}}$  from  $\hat{\pi}_\theta(\theta) \Pi_q(l_\theta(\theta) - l^*)$ 
  sample  $q_{\text{new}}$  from  $\pi_q(q) \mathbb{1}_{\{q < L_\theta(\theta_{\text{new}})/L^*\}}(\theta)$ 
  append  $(\theta_{\text{new}}, q_{\text{new}})$  to  $live\_points$ 
   $L_{\max} \leftarrow \max_{(\theta, q) \in live\_points} L(\theta, q)$ 
until  $(mass \cdot L_{\max})/Z < \epsilon$ 
 $Z_\theta \leftarrow Z/Z_q(t, q_{\max})$ 
return  $Z_\theta, dead\_points$ 

```

Sampling from $\pi_q(q) \mathbb{1}_{\{q < L_\theta(\theta_{\text{new}})/L^*\}}$ is simple. We can generate samples from $\pi_q(q)$ using inverse transform sampling [13, p. 23] as $q = \hat{\Pi}_q^{-1}(u)$ for $u \sim \text{Uniform}(0, 1)$. Using this we can generate samples until one satisfies the constraint of $q < L_\theta(\theta_{\text{new}})/L^*$. Because q is one-dimensional, we can generate millions of samples in milliseconds and need not worry about performance issues.

The q -evidence Z_q is a function of t and q_{\max} , and can be computed analytically:

$$\begin{aligned}
 Z_q(t, q_{\max}) &= \int_1^{q_{\max}} L_q(q) \pi_q(q) dq \\
 &= \int_1^{q_{\max}} \frac{\log(q)^{\frac{1}{t}-1}}{t q^2 \log(q_{\max})^{\frac{1}{t}}} dq \\
 &= \frac{1}{t \log(q_{\max})^{\frac{1}{t}}} \int_1^{q_{\max}} \frac{\log(q)^{\frac{1}{t}-1}}{q^2} dq \\
 &\stackrel{\text{int. by sub.}}{=} \frac{1}{t \log(q_{\max})^{\frac{1}{t}}} \int_0^{\log(q_{\max})} u^{\frac{1}{t}-1} e^{-u} du
 \end{aligned} \tag{2.5}$$

The substitution used is $u = \log(q)$. Now we use the definition of the lower incomplete gamma function:

$$\begin{aligned}
 \Gamma(a, x) &= \int_x^\infty u^{a-1} e^{-u} du \\
 \Gamma(a, x) - \Gamma(a, y) &= \int_x^\infty u^{a-1} e^{-u} du - \int_y^\infty u^{a-1} e^{-u} du \\
 \text{for } y > x: \quad \Gamma(a, x) - \Gamma(a, y) &= \int_x^y u^{a-1} e^{-u} du
 \end{aligned} \tag{2.6}$$

By setting $a = \frac{1}{t}$, $x = 0$ and $y = \log(q_{\max})$, we can apply (2.6) to (2.5):

$$\begin{aligned}
 Z(t, q_{\max}) &= \frac{1}{t \log(q_{\max})^{\frac{1}{t}}} \int_0^{\log(q_{\max})} u^{\frac{1}{t}-1} e^{-u} du \\
 &= \frac{\Gamma(\frac{1}{t}, 0) - \Gamma(\frac{1}{t}, \log(q_{\max}))}{t \log(q_{\max})^{\frac{1}{t}}}
 \end{aligned}$$

As implementations of the lower incomplete gamma function are readily available, this lets us easily compute Z_q to recover Z_θ from $Z_{\theta,q}$.

With that, we have successfully defined a version of Nested Sampling that incorporates the log barrier term from (2.2). Next, we will examine the newly introduced parts of the algorithm, namely the auxiliary variable q and the parameters t and q_{\max} .

2.3 Interpretation

In this section, we analyze the elements of Nested Sampling with Barriers we introduced in the previous section.

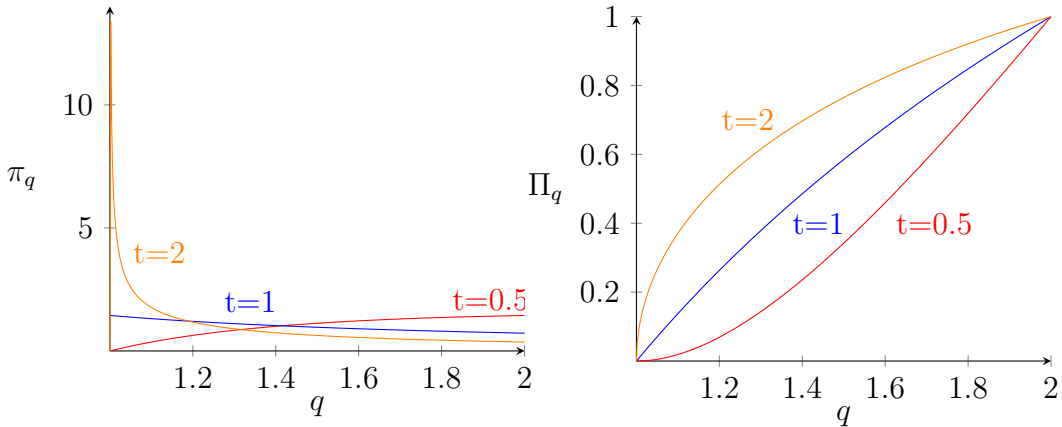


Figure 2.2: Visualization of the normalized PDF (left) and normalized CDF (right) of q for different values of t and $q_{\max} = 2$.

2.3.1 Interpreting q

Each sample from the original θ -space is paired with an auxiliary q in Nested Sampling with Barriers. Because $L(\theta, q) = \frac{L_\theta(\theta)}{q}$ and $q > 1$, the likelihood of each θ is reduced by its q . Since Z_q is divided out later, this does not influence the final evidence and is only relevant for the likelihood-threshold each point generates when it is removed from the live points. The larger the q , the more the likelihood is reduced. Since q is sampled from $\pi_q(q) \mathbb{1}_{\{q < L_\theta(\theta)/L^*\}}$, the θ that are further away from the likelihood constraint are expected to have higher q values, reducing their likelihood more. This can be interpreted as making up for the fact that the log barrier term discourages sampling close to the likelihood constraint. If the likelihoods were kept the same, the likelihood constraint would increase much more quickly.

2.3.2 Influence of t and q_{\max}

Both t and q_{\max} determine the shape and support of the distribution of q . Since the log barrier term is incorporated using the CDF of q , the two parameters also influence how the log barrier term acts.

A larger value for q_{\max} lets the log barrier term affect sampling earlier (for θ further away from the likelihood constraint boundary); a smaller q_{\max} confines the influence of the barrier term to a smaller region close to the likelihood constraint boundary. As discussed in Section 1.5, t determines how closely the log barrier approximates the true barrier. A large t leads to a better approximation, generating a steeper barrier, and making the log barrier term act less strongly in regions further away from the likelihood constraint boundary (see Figure 2.2). Lower values of t give the

log barrier term more influence even in these regions. We will see how t and q_{\max} practically influence the algorithm's performance in Chapter 3.

In the next section, we discuss, in theory, which methods for LRPS can make use of the introduced log barrier term.

2.4 Implementation of LRPS

As with the standard Nested Sampling algorithm, the step of likelihood-restricted prior sampling in the original θ -space still exists (see line 16 of Algorithm 4). However, the log barrier term now affects the sampling, which we can make use of. In this section we recapitulate the options for LRPS presented in Section 1.4 and describe how they may benefit from the log barrier term introduced by Nested Sampling with Barriers.

2.4.1 Rejection Sampling and Discretized LRPS

Because they are not MCMC methods, these techniques do not benefit from the log barrier term. Rejection Sampling proposals are not affected by the log barrier term, so their acceptance rates stay the same as with standard Nested Sampling. Discretized LRPS has no problem with acceptance rates, only with how many discrete points are needed for high-dimensional spaces, which Nested Sampling with Barriers does not help with.

2.4.2 Metropolis Algorithm

The Metropolis algorithm for LRPS can make use of the log barrier term. When a Metropolis Markov chain gets close to the likelihood constraint boundary, the log barrier term discourages it from sampling even closer. If the step size is chosen small enough, this may drastically reduce the number of invalid proposals (proposals violating the likelihood constraint). To ensure efficient exploration of the θ -space for the whole Nested Sampling procedure, an adaptive step size is still required.

2.4.3 Hamiltonian Monte Carlo

Like the Metropolis algorithm, HMC benefits from the log barrier term. It does so especially, since the log barrier term curves the negative log density surface, on which the HMC particles move, upwards as it gets closer to the likelihood constraint boundary. This causes the particles to turn away before they hit the boundary (see

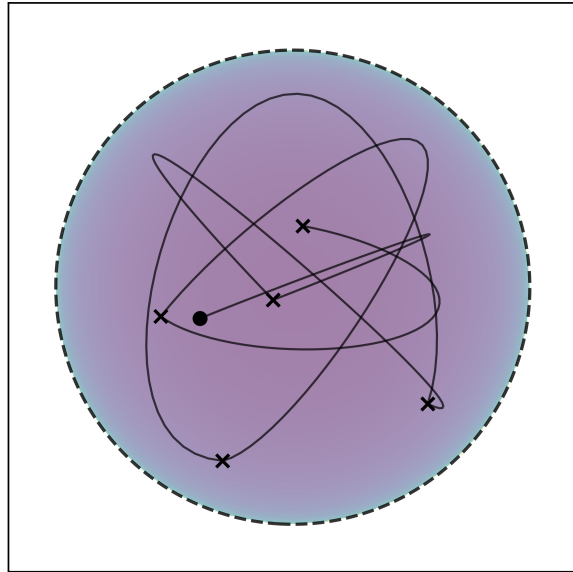


Figure 2.3: A run of HMC for LRPS with a chain of five samples on a standard-normal-likelihood-restricted uniform prior. The black dot is the starting spot, each black cross is a generated sample. The background color shows the negative log density the particles move on, with lighter colors representing higher values.

Figure 2.3), and leads to all proposals being valid. This way, the particles do not have to be reflected off the boundary. An adaptive step size is still worth implementing with this method, since the later iterations of Nested Sampling have such tiny valid spaces that the boundary may otherwise be crossed before the particle is affected by the log barrier term.

3 Results

This chapter contains the results of a number of experiments on Nested Sampling with Barriers. First, I show how Nested Sampling with Barriers compares to standard Nested Sampling using two example problems. Then, I demonstrate the influence of the parameters t and q_{\max} on Nested Sampling with Barriers on one example problem.

3.1 Nested Sampling with and without Barriers

Both standard Nested Sampling and the Barriers variant were tested on two example problems with the following likelihoods:

- $L_1(\theta) = 100 \mathcal{N}(\theta | \mu = 0, \Sigma = uI_{20}) + \mathcal{N}(\theta | \mu = 0, \Sigma = vI_{20})$
- $L_2(\theta) = 100 \mathcal{N}(\theta | \mu = (0.2, 0.2, \dots, 0.2), \Sigma = uI_{20}) + \mathcal{N}(\theta | \mu = 0, \Sigma = vI_{20})$

Where I_{20} is the 20-dimensional identity matrix, $u = 0.01$ and $v = 0.1$. Both likelihoods are two-component Gaussian mixtures consisting of a flat slab (v -component) and a thin spike with a much larger factor (u -component), and both are considered with a uniform prior on the 20-dimensional cube $[-\frac{1}{2}, \frac{1}{2}]^{20}$. The two examples are taken from Skilling's introductory paper on Nested Sampling, where the L_1 -example is presented as a type of problem Nested Sampling is well-suited for, while the L_2 -example is said to be difficult even for Nested Sampling [8, p. 21].

Since the behavior of the algorithm is heavily dependent on the method for LRPS used, I applied both standard Nested Sampling and the Barriers variant to each example problem with different LRPS methods. The following LRPS approaches were used:

- Metropolis Algorithm (with simple adaptive step size)
- HMC with reflection (only for standard Nested Sampling, with simple adaptive step size)

- HMC (only for Nested Sampling with Barriers, with simple adaptive step size)
- an optimal method for sampling inside a d -ball (only for the L_1 -problem with Standard Nested Sampling; labeled “Ball” in the figures)

We can use the optimal d -ball sampler because the valid region in the L_1 -problem is usually a ball. Only at the start, when the valid region is mostly restricted by the prior instead of the likelihood constraint, can the valid region take the shape of the prior instead of a ball. In this case, we simply reject all proposals that fall outside the prior. The sampler is taken from a paper on the topic of sphere- and ball-sampling by Voelker, Gosmann and Stewart [26, p. 2]. The simple adaptive step size Algorithm adjusts the Metropolis or HMC step size after each proposal. If the proposal is accepted, the step size is multiplied by a factor of 1.01; if it is rejected, the step size is multiplied by 0.99. The Nested Sampling configurations with Barriers use values of $t = 1$ and $q_{\max} = 2$ for their hyperparameters.

Each configuration of example problem, algorithm and LRPS method was run 200 times, with each run using 200 live points and a stopping criterion of $\epsilon = 10^{-16}$. The configurations are compared by their estimate of the evidence, how many posterior modes they find (measured in two ways), how many iterations they take, how many proposals they accept and (for the MCMC samplers) how much distance their Markov Chains cover for each proposal.

3.1.1 Estimated Evidence

In Figure 3.1, we compare how close each test run’s estimate of the evidence comes to the true value. In the concentric L_1 problem, all methods except HMC with reflection find a good estimate of the evidence. A possible explanation for the failure of HMC with reflection is as follows.

The sphere-shaped valid region of the L_1 -example causes many reflected particles to land back in the valid region, even with relatively large step sizes. This causes the adaptive step size algorithm to increase the step size even further. Eventually, the step size becomes so large that particles are always reflected into the valid region. This occurs because

- the particles are reflected not at the boundary, but at the point they would have landed at outside the valid region
- and the gradient of L_1 always points into the valid region.

These factors work together to cause highly acute angles of reflection. The behavior

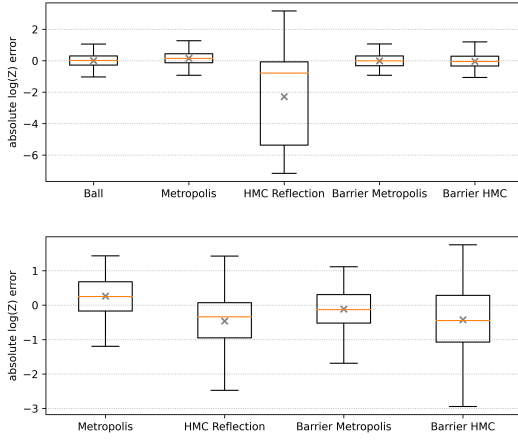


Figure 3.1: Box plot of the deviation of each method’s evidence estimate’s from the true value. Top: L_1 -example, Bottom: L_2 -example. Orange lines are the median values, gray crosses are the mean values.

is similar to the one that occurs when no adaptive step size is used, seen in Figure 1.7 of Section 1.4. This explanation of why HMC with reflection fails is backed by the fact that the runs of HMC with reflection on this example problem exhibit extremely high step sizes, up to 300 times larger than the valid region ever spans.

On the L_2 -example, none of the methods are as convincing as on the L_1 -example. The Metropolis methods are the most accurate, with the HMC methods having higher bias and higher variance. The poor performance of all methods can be explained by the next criteria, concerning how well the posterior distribution was explored.

3.1.2 Posterior Modes Found

For how well the configurations found the posterior modes, where the main challenge is finding the small spike, two criteria were implemented.

The first criterion checks, for each mode, if there is a dead point within the 95th percentile of cumulative probability of the mode, and labels the mode as found if there is. The number of modes labeled as found in this way, in proportion to how many modes there are, make up the criterion. In the upper part of Figure 3.2 on the L_1 -example, we see all methods except HMC with reflection always finding the spike. On the L_2 -example, HMC with reflection never finds the spike, with all other methods finding less than half of the time. This explains most of the bias we see in the evidence estimates.

There is a second criterion pertaining to posterior modes, which is the Kullback-Leibler divergence (KLD) of estimated and true mode weights. Here, we create an

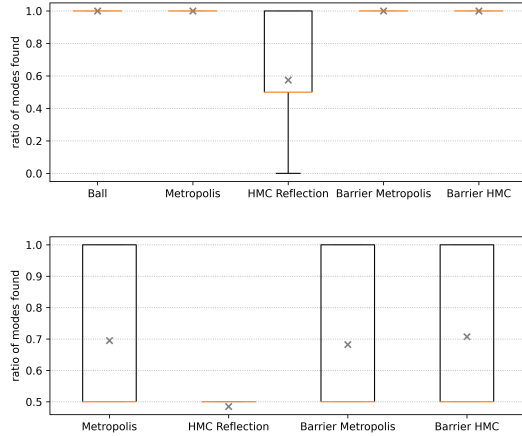


Figure 3.2: Box plots of how many of the two modes were found by each method. The values represent $\frac{m}{2}$, where m is the number of modes found. Top: L_1 -example, Bottom: L_2 -example. Orange lines are the median values, gray crosses are the mean values.

estimate of the normalized mode weights ($\frac{100}{101}$ and $\frac{1}{101}$), by evaluating the PDF of each posterior mode (only possible because both L_1 and L_2 are Gaussian mixtures) on every dead point, normalizing, multiplying by the dead points' weights and summing over all dead points. The resulting vector of mode weight estimates is again normalized and compared using the KLD to the true normalized mode weights:

$$\text{KLD}\left(\frac{\hat{m}}{\|\hat{m}\|_1}, \frac{m}{\|m\|_1}\right)$$

where $\hat{m} = \sum_i^n \frac{p(\theta_i)}{\sum_j p(\theta_j)_j} \cdot w_i$

where $p(\theta) = (\mathcal{N}_1(\theta), \mathcal{N}_2(\theta))$

With \mathcal{N}_1 and \mathcal{N}_2 being the unweighted mode PDFs, $\theta_1, \dots, \theta_n$ being the dead points, w_1, \dots, w_n being the dead points' estimated prior mass shells, m being the vector of true mode weights, $(100, 1)$ and $\|\cdot\|_1$ being the L^1 -Norm: $\|x\|_1 = \sum_i |x_i|$.

The results in Figure 3.3 show a similar pattern to the evidence estimate results. In the L_1 -example, all methods but HMC with reflection are nearly equal and, in relation to the optimal ball sampler's performance, almost perfect. In the L_2 -example, the Metropolis methods tend to be worse than the HMC methods, but the HMC methods have higher variance.

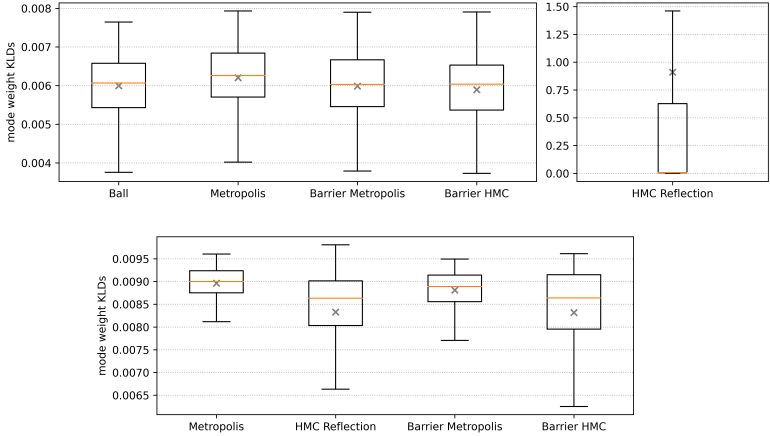


Figure 3.3: Box plots of the KLD of estimated and true mode weights. Top: L_1 -example, Bottom: L_2 -example. The results for HMC with reflection are presented on a separate scale to enable better comparison between the others. Orange lines are the median values, gray crosses are the mean values.

3.1.3 Number of Iterations

Figure 3.4 shows how many iterations each configuration took to accumulate enough of the evidence to satisfy the stopping criterion of $\epsilon = 10^{-16}$. For the L_1 -example, HMC with reflection is again the outlier, showing drastically more variance than the other methods. For both L_1 and L_2 , the non-barrier methods take slightly fewer iterations than the barrier methods, and the Metropolis approach has lower variance than the HMC approaches.

3.1.4 Acceptance Rate

In this section, we examine what ratio of the total proposals made during LRPS are accepted. Lower acceptance rates lead to slower overall execution time as more proposals have to be made until an acceptable one is found. As is visible in Figure 3.5, this is where the main advantage of Nested Sampling with Barriers lies. In both example problems, Nested Sampling with Barriers reaches significantly higher acceptance rates than standard Nested Sampling when both use the Metropolis algorithm. For the L_1 -example, the version with barriers achieves an acceptance rate that is a factor of 1.62 higher than the standard version's acceptance rate. In the L_2 -example, the improvement is by a factor of 1.23. The HMC methods are completely even, and, as one would expect, the optimal sampler reaches the highest proposal acceptance rate. The reason the optimal sampler does not reach an acceptance rate of 1 is that in the early iterations, the likelihood constraint boundary

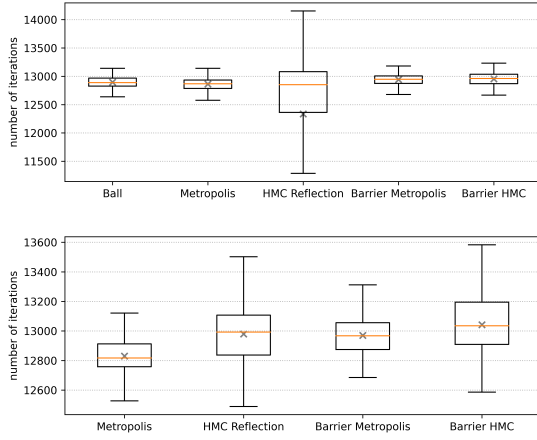


Figure 3.4: Box plots of how many iterations each method took to reach the stopping point. Top: L_1 -example, Bottom: L_2 -example. Orange lines are the median values, gray crosses are the mean values.

is further outwards from the origin than the prior reaches, causing a significant number of early proposals to be rejected because they do not land in the prior.

3.1.5 Jump Distance

Because all tested MCMC methods use an adaptive step size, just examining the acceptance rate does not present the full picture. For the HMC methods, the adaptive step size keeps the acceptance rate steadily at 0.5, so we have to look at how much the step size has to be reduced to achieve this acceptance rate. The step size, however, is just how far each singular MCMC step goes. We are instead interested in how long the whole Markov Chain from one sample to the next is. This criterion is called the jump distance [27].

In Figure 3.6, we see how the mean jump distance per iteration develops for each configuration. The barrier versions of the algorithms start out with lower jump distances than their standard counterparts, but in the late iterations, when sampling becomes difficult, they actually have higher jump distances. The curve of HMC with reflection ends earlier than the others in the L_1 -example because its number of iterations varies much more than the others and the curves are only shown as far as the shortest run of each configuration went.

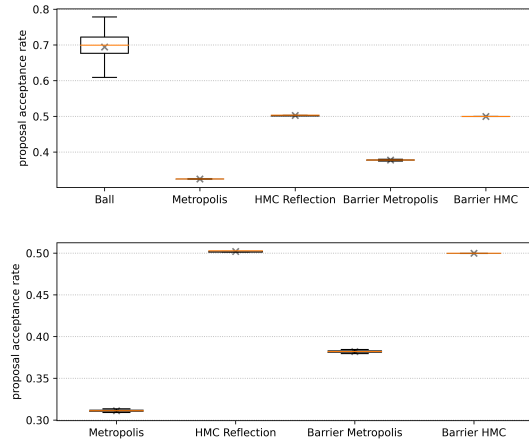


Figure 3.5: Box plots of the ratio of accepted proposals to total proposals made during LRPS for each method. Top: L_1 -example, Bottom: L_2 -example. Orange lines are the median values, gray crosses are the mean values.

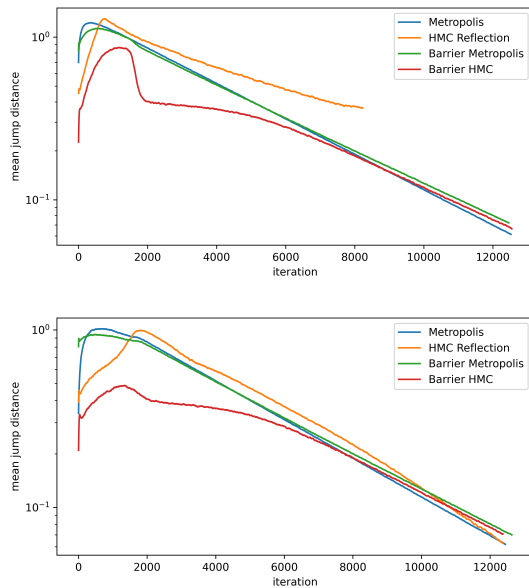


Figure 3.6: Mean jump distance of each configuration per iteration; Unweighted rolling average with a window of 50. Top: L_1 -example, Bottom: L_2 -example. Curves are only shown as far as the shortest run went.

3.2 Influence of t and q_{\max}

In this section, we examine the influence of the hyperparameters t and q_{\max} which Nested Sampling with Barriers introduces. 0.5, 1, 2, and 5 were used as values for t and 1, 1.1, 2 and 5 as values for q_{\max} . Each combination of t and q_{\max} values was used in two configuration of Nested Sampling with Barriers, one using Metropolis for LRPS and one using HMC. These configurations, each using 200 live points and a stopping criterion of $\epsilon = 10^{-16}$, were applied to the L_2 -problem introduced in the previous section. The results of 200 runs per configuration are compiled in the following paragraphs.

3.2.1 Estimated Evidence

As is visible in Figure 3.7, the evidence estimates are barely affected by the choice of t and q_{\max} . For the HMC version, $q_{\max} = 1.1$ causes higher variance in the estimates than other values. In both the Metropolis and the HMC versions, the value of q_{\max} has no discernible impact.

3.2.2 Posterior Modes Found

Figure 3.8 shows the number of modes found by each configuration, while Figure 3.9 shows the KLD of the estimated and true mode weights. While some configurations, like $t = 0.5, q_{\max} = 2$ for the Metropolis example, have a slightly higher mean number of modes found, there is no discernible pattern to these fluctuations. The KLDs are mostly stable across configurations, except for the $q_{\max} = 1.1$ versions using HMC, which have higher variance than the other configurations. The configuration with $t = 5, q_{\max} = 1.1$ is especially problematic, with large outliers bringing its mean KLD far above the median.

3.2.3 Number of Iterations

With the number of iterations, seen in Figure 3.10, there is a trend of higher values of t causing slightly fewer iterations to be needed, while higher values of q_{\max} have the opposite effect.

3.2.4 Acceptance Rate

The acceptance rates, visible in Figure 3.11, show differing trends for the Metropolis and the HMC version. For the Metropolis version, higher values of t lead to

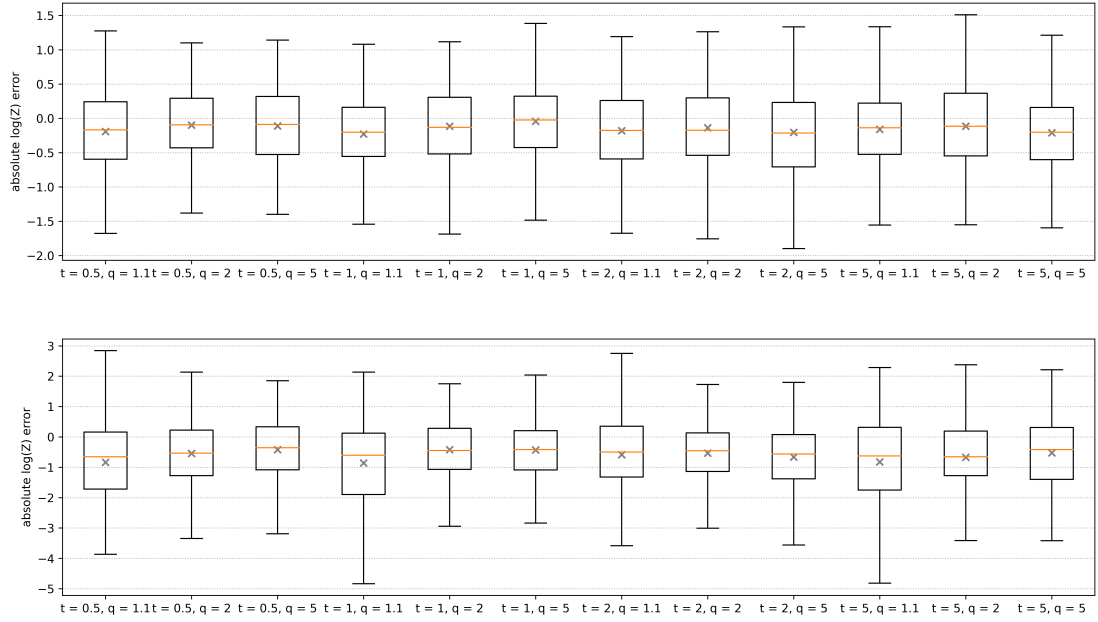


Figure 3.7: Box plot of each configuration's evidence estimate's deviation from the true value. Top: Using Metropolis for LPRS, Bottom: Using HMC for LRPS. Orange lines are the median values, gray crosses are the mean values.

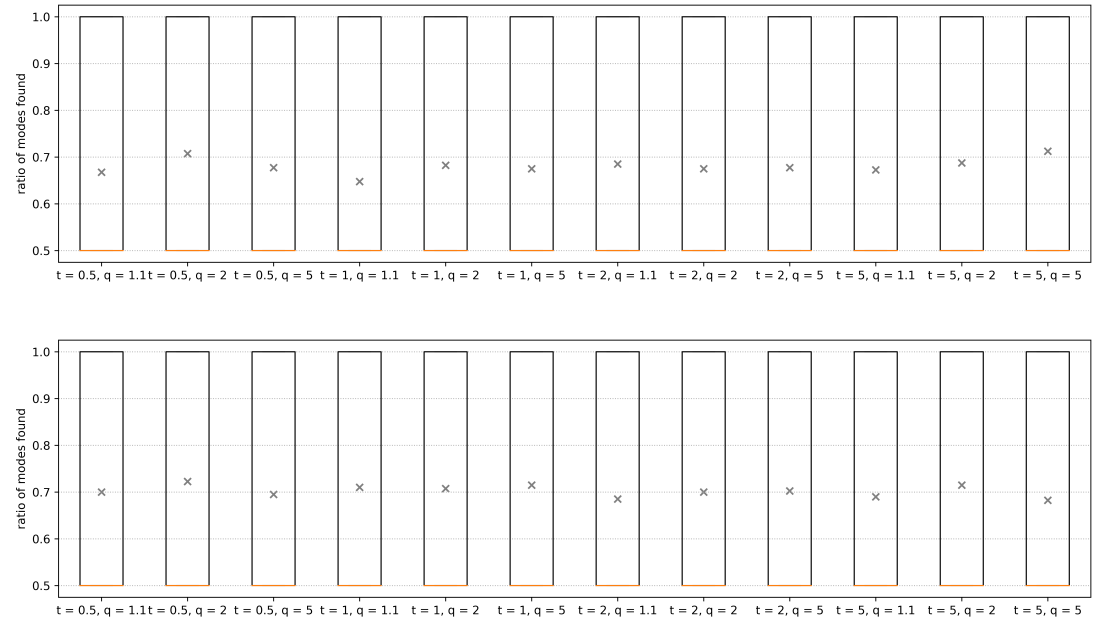


Figure 3.8: Box plots of how many of the two modes were found by each method. The values represent $\frac{m}{2}$, where m is the number of modes found. Top: Using Metropolis for LPRS, Bottom: Using HMC for LRPS. Orange lines are the median values, gray crosses are the mean values.

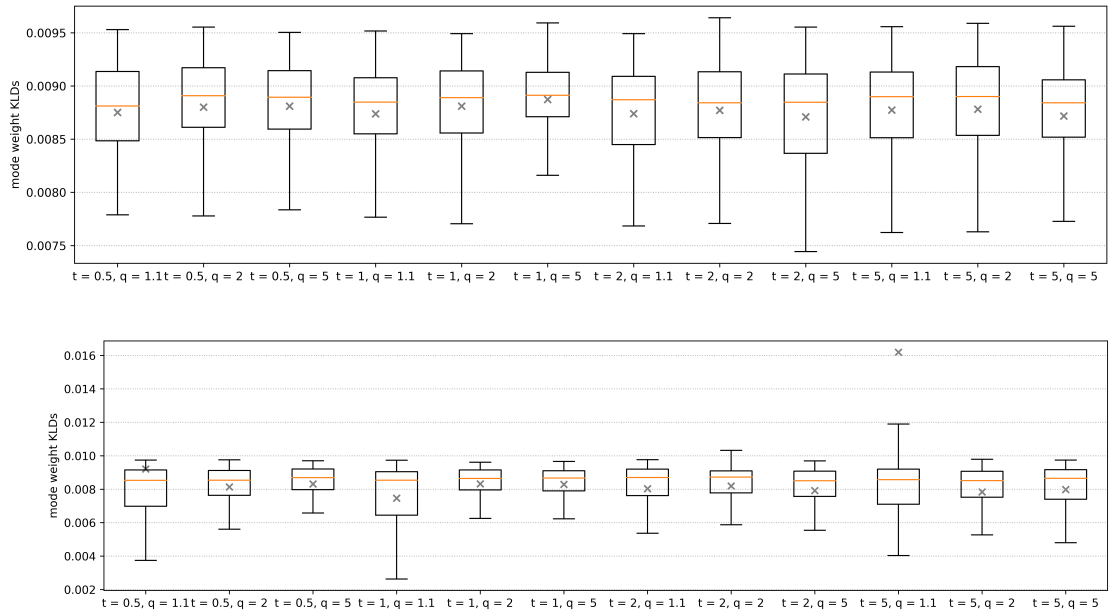


Figure 3.9: Box plots of the KLD of estimated and true mode weights. Top: Using Metropolis for LPRS, Bottom: Using HMC for LPRS. Orange lines are the median values, gray crosses are the mean values.

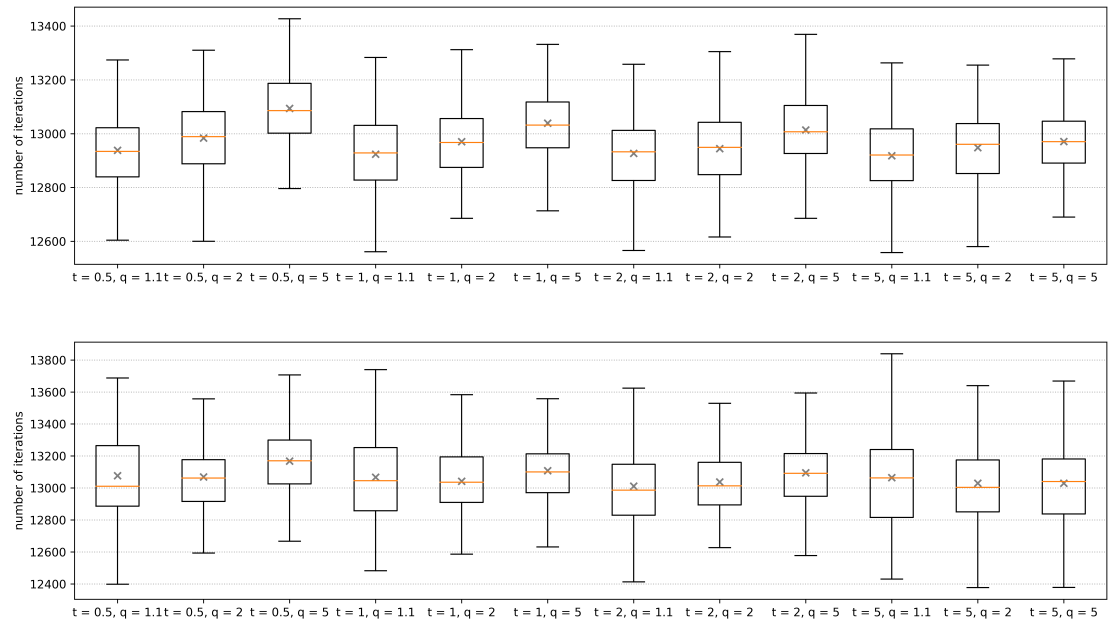


Figure 3.10: Box plots of how many iterations each configuration took to reach the stopping point. Top: Using Metropolis for LPRS, Bottom: Using HMC for LPRS. Orange lines are the median values, gray crosses are the mean values.

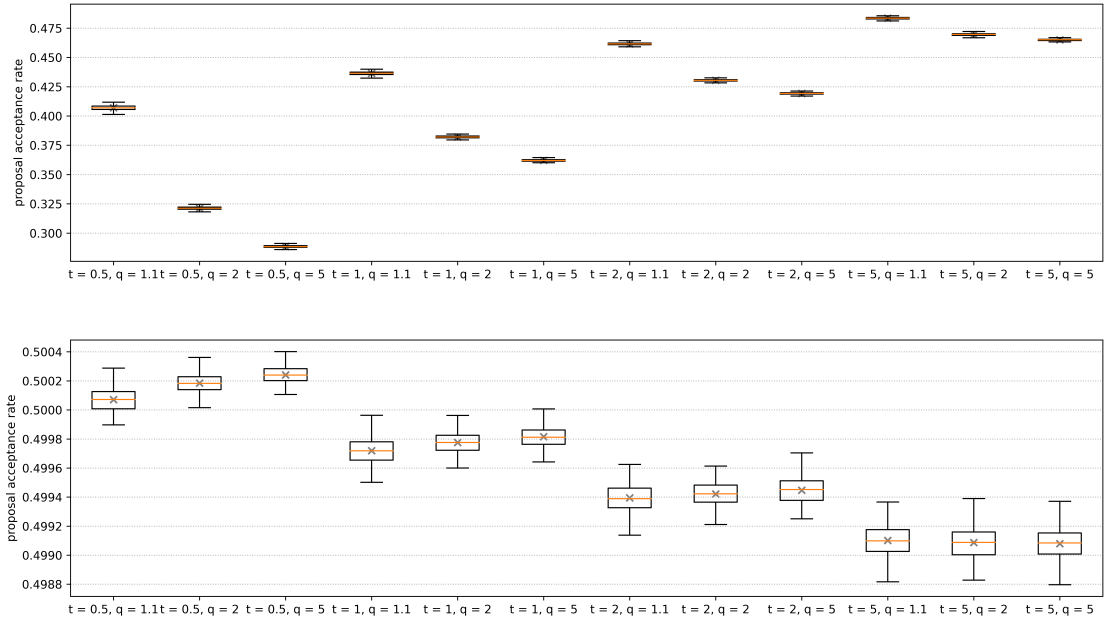


Figure 3.11: Box plots of the ratio of accepted proposals to total proposals made during LRPS for each configuration. Top: Using Metropolis for LPRS, Bottom: Using HMC for LRPS. Orange lines are the median values, gray crosses are the mean values.

significantly higher mean acceptance rates, with an increase by a factor of 1.67 from the configuration with $t = 0.5, q_{\max} = 5$ to the configuration with $t = 5, q_{\max} = 1.1$. In the HMC version, this trend is reversed, with higher values of t causing lower acceptance rates, although at a much lower scale, with the $t = 0.5, q_{\max} = 5$ configuration beating the $t = 5, q_{\max} = 5$ configuration by a factor of only 1.002. In both cases, q_{\max} 's influence is opposite of t and stronger for lower values of t .

3.2.5 Jump Distance

For the Metropolis version in Figure 3.12, the value of t has no discernible impact. The configurations with higher values of q_{\max} have higher jump distances over all iterations. In the HMC version in Figure 3.13, both parameters have much more influence on the jump distances. Lower values of t lead to higher jump distances, but also to larger differences between configurations with different values of q_{\max} . Again, higher values of q_{\max} cause higher jump distances over the whole run.

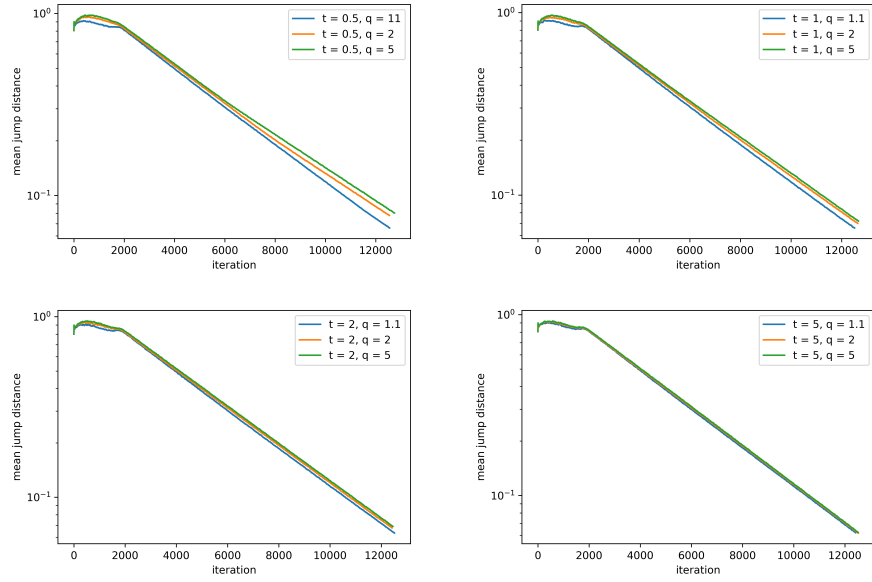


Figure 3.12: Mean jump distance of each Metropolis configuration per iteration.

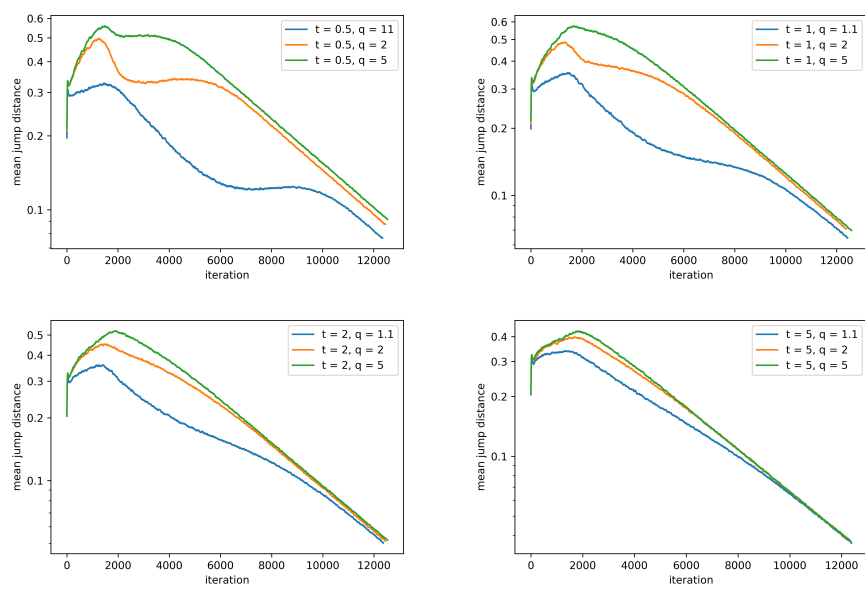


Figure 3.13: Mean jump distance of each HMC configuration per iteration.

4 Conclusions

This thesis introduced Nested Sampling with Barriers as a modification of the standard Nested Sampling algorithm that softens the hard likelihood constraint boundary and guides MCMC samplers during the LRPS step. Using the Metropolis algorithm for LRPS, it achieves mean acceptance rates that are up to a factor of 1.23 higher than standard Nested Sampling. Using HMC for LRPS, it reaches higher jump distances than standard Nested Sampling in the later iterations, but sacrifices jump distance in the early iterations of a run. Other criteria such as correctness of evidence estimates, number of posterior modes found and number of iterations taken stay largely the same as with standard Nested Sampling. These results indicate that Nested Sampling with Barriers is able to effectively guide the LRPS sampler to explore the posterior more efficiently without sacrificing performance in other ways.

Even though these results show promise, the example problems they were achieved on are quite simple. The performance of Nested Sampling with Barriers on problems with

- more than two modes,
- more than twenty parameters,
- likelihoods of higher complexity than isometric Gaussians, and
- non-uniform priors

is yet to be determined, which leaves its practical use cases uncertain. Future research could benchmark Nested Sampling with Barriers on such problems, comparing it to state-of-the-art implementations of Nested Sampling like UltraNest [28], dynesty [29], JAXNS [30], and PolyChord [31]. Many of the ideas used by these implementations, like the dynamic number of live points from dynesty or the complex adaptive step size of UltraNest could also be applied to Nested Sampling. Furthermore, the convergence rate of Nested Sampling with Barriers warrants thorough theoretical investigation. The derivation of Nested Sampling itself, especially the reformulation of the evidence

as a one-dimensional integral, also shows room for more research. The theory could be formalized and put on rigorous foundations using measure theory. Another point of interest is the curious behavior of jump distances in Nested Sampling with Barriers, outperforming standard Nested Sampling in the late iterations of the run while sacrificing jump distance in the early iterations.

Bibliography

- [1] George Casella and Edward George. “Explaning the Gibbs Sampler”. In: *The American Statistician* 46 (Aug. 1992), pp. 167–174. DOI: [10.1080/00031305.1992.10475878](https://doi.org/10.1080/00031305.1992.10475878).
- [2] Nicholas Metropolis et al. *Equation of State Calculations by Fast Computing Machines*. 1953.
- [3] Simon Duane et al. “Hybrid Monte Carlo”. In: *Physics Letters B* 195.2 (1987), pp. 216–222. ISSN: 0370-2693. DOI: [https://doi.org/10.1016/0370-2693\(87\)91197-X](https://doi.org/10.1016/0370-2693(87)91197-X). URL: <https://www.sciencedirect.com/science/article/pii/037026938791197X>.
- [4] Radford M. Neal. “Slice sampling”. In: *The Annals of Statistics* 31.3 (2003), pp. 705–767. DOI: [10.1214/aos/1056562461](https://doi.org/10.1214/aos/1056562461).
- [5] Radford M. Neal. *Annealed Importance Sampling*. 1998. arXiv: [physics/9803008](https://arxiv.org/abs/physics/9803008) [physics.comp-ph].
- [6] Andrew Gelman and Xiao-Li Meng. “Simulating normalizing constants: from importance sampling to bridge sampling to path sampling”. In: *Statistical Science* 13.2 (1998), pp. 163–185. DOI: [10.1214/ss/1028905934](https://doi.org/10.1214/ss/1028905934). URL: <https://doi.org/10.1214/ss/1028905934>.
- [7] François-Xavier Briol et al. *Probabilistic Integration: A Role in Statistical Computation?* 2017. arXiv: [1512.00933](https://arxiv.org/abs/1512.00933) [stat.ML].
- [8] John Skilling. “Nested sampling for general Bayesian computation”. In: *Bayesian Analysis* 1.4 (2006), pp. 833–859. DOI: [10.1214/06-BA127](https://doi.org/10.1214/06-BA127).
- [9] Michael Betancourt et al. “Nested Sampling with Constrained Hamiltonian Monte Carlo”. In: *AIP Conference Proceedings*. AIP, 2011. DOI: [10.1063/1.3573613](https://doi.org/10.1063/1.3573613).
- [10] E. T. Jaynes. *Probability Theory: The Logic of Science*. Ed. by G. Larry Bretthorst. Cambridge University Press, 2003.
- [11] Richard McElreath. *Statistical Rethinking*. 2nd. CRC Press, 2020. ISBN: 978-0-367-13991-9.

- [12] David J. C. MacKay. *Information Theory, Inference & Learning Algorithms*. USA: Cambridge University Press, 2002. ISBN: 0521642981.
- [13] Andrew Gelman et al. *Bayesian Data Analysis*. 3rd ed. CRC Press, 2021.
- [14] Michael Betancourt. *Efficient Bayesian Inference with Hamiltonian Monte Carlo*. Talk at the Machine Learning Summer School of the Reykjavik University. Apr. 29, 2014.
- [15] Elliot H Lieb and Michael Loss. *Analysis*. 2nd. American Mathematical Society, 2001.
- [16] Donald L. Cohn. *Measure Theory*. 2nd. Birkhäuser New York, 2013.
- [17] George Casella and Roger Berger. *Statistical Inference*. 2nd. CRC Press, 2024.
- [18] James E. Gentle. *Computational Statistics*. 1st. Springer New York, 2009.
- [19] Kyle Siegrist. *Probability, Mathematical Statistics, and Stochastic Processes*. LibreTexts, 2022.
- [20] Will Handley. *Gradients and Nested Sampling*. Invited talk at MIAPbP. July 7, 2023.
- [21] Solomon Kullback. *Information Theory and Statistics*. Dover Publications, 1968.
- [22] Miguel Biron-Lattes et al. *autoMALA: Locally adaptive Metropolis-adjusted Langevin algorithm*. 2024. arXiv: 2310.16782 [stat.CO].
- [23] Michael Betancourt. *A Conceptual Introduction to Hamiltonian Monte Carlo*. 2018. arXiv: 1701.02434 [stat.ME].
- [24] Stephen Boyd and Lieven Vandenberghe. *Convex Optimization*. Cambridge University Press, 2004.
- [25] Jun S. Liu. “The Collapsed Gibbs Sampler in Bayesian Computations with Applications to a Gene Regulation Problem”. In: *Journal of the American Statistical Association* 89.427 (1994), pp. 958–966. DOI: 10.1080/01621459.1994.10476829.
- [26] Aaron R. Voelker, Jan Gosmann, and Terrence C. Stewart. “Efficiently sampling vectors and coordinates from the n-sphere and n-ball”. In: *Centre for Theoretical Neuroscience* (2017).
- [27] Johannes Buchner. *Relative Jump Distance: a diagnostic for Nested Sampling*. 2024. arXiv: 2402.11936 [stat.ME]. URL: <https://arxiv.org/abs/2402.11936>.
- [28] Johannes Buchner. *UltraNest – a robust, general purpose Bayesian inference engine*. 2021. arXiv: 2101.09604 [stat.CO]. URL: <https://arxiv.org/abs/2101.09604>.

- [29] Joshua S Speagle. “dynesty: a dynamic nested sampling package for estimating Bayesian posteriors and evidences”. In: *Monthly Notices of the Royal Astronomical Society* 493.3 (Feb. 2020), pp. 3132–3158. ISSN: 1365-2966. DOI: 10.1093/mnras/staa278. URL: <http://dx.doi.org/10.1093/mnras/staa278>.
- [30] Joshua G. Albert. *JAXNS: a high-performance nested sampling package based on JAX*. 2020. arXiv: 2012.15286 [astro-ph.IM]. URL: <https://arxiv.org/abs/2012.15286>.
- [31] W. J. Handley, M. P. Hobson, and A. N. Lasenby. “polychord: next-generation nested sampling”. In: *Monthly Notices of the Royal Astronomical Society* 453.4 (Sept. 2015), pp. 4385–4399. ISSN: 1365-2966. DOI: 10.1093/mnras/stv1911. URL: <http://dx.doi.org/10.1093/mnras/stv1911>.

Appendix

Proof: LRPS Samples' Prior Masses are Uniformly Distributed

Let \mathbb{T} be a random variable with $f_T(\theta) = \pi(\theta) \mathbb{1}_{\{L(\theta)>L^*\}}(\theta)$. Let $\mathbb{L} = L(\mathbb{T})$ and $\mathbb{M} = \mu(\mathbb{L})$. \mathbb{M} represents the prior masses, we want to prove that it follows a uniform distribution. Because we are dealing with a likelihood-restricted prior, the uniform distribution is not on $[0, 1]$, but on $[0, \mu(L^*)]$.

$$f_{\mathbb{L}}(\lambda) = \int_{\Theta} \delta(\lambda - L(\theta)) \pi(\theta) \mathbb{1}_{\{L(\theta)>L^*\}}(\theta) d\theta,$$

Plugging the PDF-formula into the CDF:

$$\begin{aligned} F_{\mathbb{L}}(\lambda) &= \int_0^\lambda f_{\mathbb{L}}(\lambda') \mathbb{1}_{\{L(\theta)>L^*\}}(\theta) d\lambda' \\ &= \int_0^\lambda \int_{\Theta} \pi(\theta) \mathbb{1}_{\{L(\theta)>L^*\}}(\theta) \delta(\lambda' - L(\theta)) d\theta d\lambda' \\ &= \int_{\Theta} \int_0^\lambda \pi(\theta) \mathbb{1}_{\{L(\theta)>L^*\}}(\theta) \delta(\lambda' - L(\theta)) d\lambda' d\theta \\ &= \int_{\Theta} \pi(\theta) \mathbb{1}_{\{L(\theta)>L^*\}}(\theta) \int_0^\lambda \delta(\lambda' - L(\theta)) d\lambda' d\theta \\ &= \int_{\Theta} \pi(\theta) \mathbb{1}_{\{L(\theta)>L^*\}}(\theta) \mathbb{1}_{\{L(\theta)<\lambda\}}(\theta) d\theta \\ &= \int_{\{L^*<L(\theta)<\lambda\}} \pi(\theta) d\theta \\ &= \mu(L^*) - \mu(\lambda) \end{aligned} \tag{4.1}$$

See also the visualization for the last step in Figure 4.1.

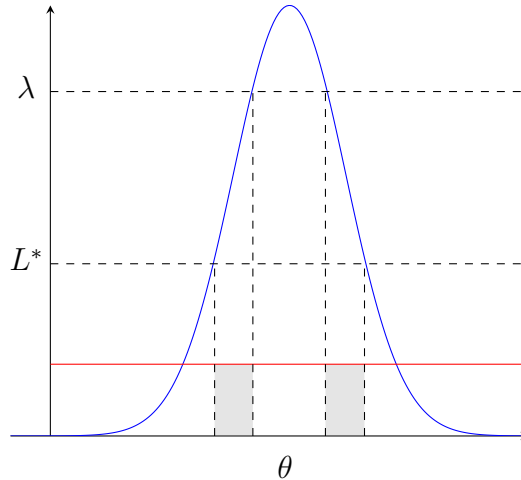


Figure 4.1: Visualization of the integral in (4.1). The shaded region is the integral, equivalent to $\mu(L^*) - \mu(\lambda)$.

$\mathbb{Y} = f(\mathbb{X})$ is uniform if f is the CDF of \mathbb{X} [17, p. 54]. This means that $\overline{\mathbb{M}} = \mu(L^*) - \mu(\mathbb{L})$ would be uniformly distributed on $[0, \mu(L^*)]$, since $\mu(L^*) - \mu(\lambda)$ is the CDF of \mathbb{L} . And since \mathbb{M} 's values are simply the values of $\overline{\mathbb{M}}$ mirrored, \mathbb{M} is also uniformly distributed. \square

Declaration of Academic Integrity

1. I hereby confirm that this work — or in case of group work, the contribution for which I am responsible and which I have clearly identified as such — is my own work and that I have not used any sources or resources other than those referenced. I take responsibility for the quality of this text and its content and have ensured that all information and arguments provided are substantiated with or supported by appropriate academic sources. I have clearly identified and fully referenced any material such as text passages, thoughts, concepts or graphics that I have directly or indirectly copied from the work of others or my own previous work. Except where stated otherwise by reference or acknowledgement, the work presented is my own in terms of copyright.
2. I understand that this declaration also applies to generative AI tools which cannot be cited (hereinafter referred to as ‘generative AI’). I understand that the use of generative AI is not permitted unless the examiner has explicitly authorized its use (Declaration of Permitted Resources). Where the use of generative AI was permitted, I confirm that I have only used it as a resource and that this work is largely my own original work. I take full responsibility for any AI-generated content I included in my work. Where the use of generative AI was permitted to compose this work, I have acknowledged its use in a separate appendix. This appendix includes information about which AI tool was used or a detailed description of how it was used in accordance with the requirements specified in the examiner’s Declaration of Permitted Resources. I have read and understood the requirements contained therein and any use of generative AI in this work has been acknowledged accordingly (e.g. type, purpose and scope as well as specific instructions on how to acknowledge its use).
3. I also confirm that this work has not been previously submitted in an identical or similar form to any other examination authority in Germany or abroad, and that it has not been previously published in German or any other language.
4. I am aware that any failure to observe the aforementioned points may lead to the imposition of penalties in accordance with the relevant examination regulations. In particular, this may include that my work will be classified as deception and marked as failed. Repeated or severe attempts to deceive may also lead to a temporary or permanent exclusion from further assessments in my degree program.